

## **Supplementary Information:**

### **Primary Coloured Electrochromism of Aromatic Oxygen and Sulfur Diesters**

Xiuhui Xu, Richard D. Webster\*

*Division of Chemistry and Biology Chemistry, School of Physical & Mathematical  
Sciences, Nanyang Technological University, Singapore  
21 Nanyang Link, Singapore 637371.*

[webster@ntu.edu.sg](mailto:webster@ntu.edu.sg)

## Table of Contents

	Page
1. General Experimental Information	S4
2. Experimental Procedure for the Preparation of <i>S,S</i> -diethyl esters	S4
3. Experimental Procedure for the Preparation of <i>O</i> -diesters	S5
4. Spectroscopic Data	
A. <sup>1</sup> H and <sup>13</sup> C NMR spectra	S8
i. Compound <b>1</b> - <i>S,S</i> -Diethyl benzene-1,4-bis(carbothioate)	S8
ii. Compound <b>2</b> - <i>S,S</i> -Diethyl pyridine-2,5-bis(carbothioate)	S9
iii. Compound <b>3</b> - Dimethyl terephthalate	S10
iv. Compound <b>4</b> - Dimethyl pyridine-2,5-dicarboxylate	S11
v. Compound <b>5</b> - Diisopropyl terephthalate	S12
vi. Compound <b>6</b> - Diisopropyl pyridine-2,5-dicarboxylate	S13
vii. Compound <b>7</b> - Dipropyl terephthalate	S14
viii. Compound <b>8</b> - Dipropyl pyridine-2,5-dicarboxylate	S15
ix. Compound <b>9</b> - Dimethyl naphthalene-2,6-dicarboxylate	S16
x. Compound <b>10</b> - Dimethyl biphenyl-4,4'-dicarboxylate	S17
xi. Compound <b>11</b> - Dimethyl [2,2'-bipyridine]-5,5'-dicarboxylate	S18
B. Cyclic voltammograms (varying scan rates) at 22 °C and -30°C	S19
i. Compound <b>1</b> - <i>S,S</i> -Diethyl benzene-1,4-bis(carbothioate)	S19
ii. Compound <b>2</b> - <i>S,S</i> -Diethyl pyridine-2,5-bis(carbothioate)	S20
iii. Compound <b>3</b> - Dimethyl terephthalate	S21
iv. Compound <b>4</b> - Dimethyl pyridine-2,5-dicarboxylate	S22
v. Compound <b>5</b> - Diisopropyl terephthalate	S23
vi. Compound <b>6</b> - Diisopropyl pyridine-2,5-dicarboxylate	S24
vii. Compound <b>7</b> - Dipropyl terephthalate	S25
viii. Compound <b>8</b> - Dipropyl pyridine-2,5-dicarboxylate	S26
ix. Compound <b>9</b> - Dimethyl naphthalene-2,6-dicarboxylate	S27
x. Compound <b>10</b> - Dimethyl biphenyl-4,4'-dicarboxylate	S28
xi. Compound <b>11</b> - Dimethyl [2,2'-bipyridine]-5,5'-dicarboxylate	S29
C. Voltammetric and coulometric spectra during electrolysis	S30
i. Compound <b>1</b> - <i>S,S</i> -Diethyl benzene-1,4-bis(carbothioate)	S30
ii. Compound <b>2</b> - <i>S,S</i> -Diethyl pyridine-2,5-bis(carbothioate)	S31
iii. Compound <b>3</b> - Dimethyl terephthalate	S32
iv. Compound <b>4</b> - Dimethyl pyridine-2,5-dicarboxylate	S33
v. Compound <b>5</b> - Diisopropyl terephthalate	S34
vi. Compound <b>6</b> - Diisopropyl pyridine-2,5-dicarboxylate	S35
vii. Compound <b>7</b> - Dipropyl terephthalate	S36
viii. Compound <b>8</b> - Dipropyl pyridine-2,5-dicarboxylate	S37
ix. Compound <b>9</b> - Dimethyl naphthalene-2,6-dicarboxylate	S38

D.	<i>In situ</i> electrochemical UV-vis spectra at Pt mesh electrode	S39
i.	Compound <b>1</b> - <i>S,S</i> -Diethyl benzene-1,4-bis(carbothioate)	S39
ii.	Compound <b>2</b> - <i>S,S</i> -Diethyl pyridine-2,5-bis(carbothioate)	S39
iii.	Compound <b>3</b> - Dimethyl terephthalate	S40
iv.	Compound <b>4</b> - Dimethyl pyridine-2,5-dicarboxylate	S40
v.	Compound <b>5</b> - Diisopropyl terephthalate	S41
vi.	Compound <b>6</b> - Diisopropyl pyridine-2,5-dicarboxylate	S41
vii.	Compound <b>7</b> - Dipropyl terephthalate	S42
viii.	Compound <b>8</b> - Dipropyl pyridine-2,5-dicarboxylate	S42
ix.	Compound <b>9</b> - Dimethyl naphthalene-2,6-dicarboxylate	S43
E.	Voltammetric and UV-vis spectra using gold-mesh electrode	
i.	<i>In situ</i> electrochemical UV-vis spectra of Compound <b>2</b>	S44
ii.	<i>In situ</i> electrochemical UV-vis spectra of Compound <b>5</b>	S44
iii.	<i>In situ</i> electrochemical UV-vis spectra of Compound <b>9</b>	S45
iv.	Absorbance spectrum of gold-mesh electrode	S45
v.	Table of chromatic contrast ratios of compounds <b>2</b> , <b>5</b> and <b>9</b>	S46
vi.	Coulometric data obtained from LSV of compounds <b>2</b> , <b>5</b> and <b>9</b>	S47
vii.	Table of chromatic efficiencies of compounds <b>2</b> , <b>5</b> and <b>9</b>	S48
viii.	100 cycles of cyclic voltammograms of Compound <b>2</b>	S48
ix.	100 cycles of cyclic voltammograms of Compound <b>5</b>	S49
x.	100 cycles of cyclic voltammograms of Compound <b>9</b>	S49

## General Experimental Information

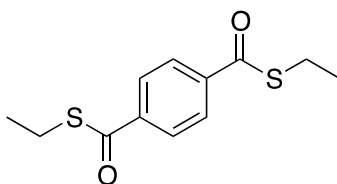
Unless specified, all reagents and starting materials were purchased from commercial sources and used as received. Solvents were purified following standard literature procedures. Analytical thin layer chromatography (TLC) was performed using pre-coated silica gel plates. Visualization was achieved by UV light (254 nm). Flash chromatography was performed using silica gel and gradient solvent system (EtOAc:nHexane as eluent).  $^1\text{H}$  and  $^{13}\text{C}$  NMR spectra were recorded with 400 MHz spectrometer. Chemical shifts (ppm) were recorded with tetramethylsilane (TMS) as the internal reference standard. Multiplicities are given as: s (singlet), br s (broad singlet), d (doublet), t (triplet), dd (doublet of doublets), q (quartet) or m (multiplet). The number of protons (**n**) for a given resonance is indicated by **nH** and coupling constants are reported as a **J** value in Hz. Infrared spectra were recorded on a IR spectrometer. Solid samples were examined as a thin film between NaCl salt plates. Low resolution mass spectra were determined on a mass spectrometer and reported in units of mass to charge (**m/z**). High-resolution mass spectra (HRMS) were obtained on a LC/HRMS mass spectrometer.

## General Procedure for the Preparation of *S,S*-diethyl esters

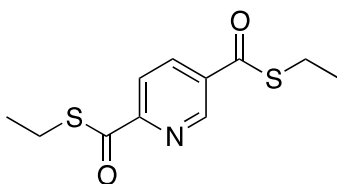
Compounds (**1** & **2**)

To 15 mmol of the dicarboxylic acid, 10 ml of thionyl chloride was added and reflux in DMF for 3 hours. Triethylamine and ethanethiol were then added, followed by dry THF and left to reflux overnight. Upon completion of reaction, solvent was removed under reduced pressure. Mixture was washed with sodium bicarbonate and extracted twice with ether. Combined organic layers were dried with sodium sulfate. Organic layer was then dried under reduced pressure to yield the final product.

## Spectroscopic data



*S,S*-diethyl benzene-1,4-bis(carbothioate) (**1**): White solid; mp: 88-91 °C; IR (Nujol) 1668 (S–C=O)  $\text{cm}^{-1}$ ;  $^1\text{H}$  NMR ( $\text{CDCl}_3$ , 400 MHz)  $\delta$  8.01 (s, 4H), 3.95 (q, 2H,  $J = 7.44$  Hz), 1.35 (t, 3H,  $J = 7.44$  Hz);  $^{13}\text{C}$  NMR ( $\text{CDCl}_3$ , 400 MHz)  $\delta$  191.4, 140.6, 127.4, 23.8, 14.6; HRMS ESI ( $m/z$ ): found, 255.0517, calcd for  $\text{C}_{12}\text{H}_{15}\text{O}_4\text{S}_2$ :  $[\text{M}+\text{H}]^+$ , 255.0513.



*S,S*-diethyl pyridine-2,5-bis(carbothioate) (**2**): Pale-yellow solid; mp: 88-90 °C; IR (Nujol) 1667 (S–C=O)  $\text{cm}^{-1}$ ;  $^1\text{H}$  NMR ( $\text{CDCl}_3$ , 400 MHz)  $\delta$  9.19 (d, 1H,  $J = 1.96$  Hz), 8.32 (dd, 1H,  $J = 8.12, 2.12$  Hz), 8.02 (d, 1H,  $J = 8.04$  Hz), 3.11 (q, 2H,  $J = 7.44$

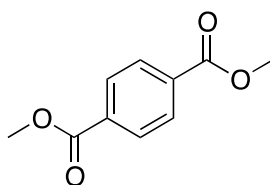
Hz), 3.04 (q, 2H,  $J = 7.44$  Hz), 1.34 (q, 6H,  $J = 7.52$  Hz);  $^{13}\text{C}$  NMR ( $\text{CDCl}_3$ , 400 MHz)  $\delta$  192.9, 189.9, 154.6, 147.8, 135.9, 135.6, 120.1, 23.9, 23.3, 14.5, 14.3; HRMS ESI ( $m/z$ ): found, 256.0471, calcd for  $\text{C}_{11}\text{H}_{14}\text{NO}_2\text{S}_2$ :  $[\text{M}+\text{H}]^+$ , 256.0466.

### General Procedure for the Preparation of *O*-diesters

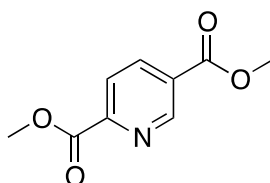
Compounds (**3** - **11**)

To 3 mmol of the dicarboxylic acid, approximately 0.5 ml of concentrated Sulfuric acid was added and reflux in its respective alcohol overnight. Upon completion of reaction, solvent was removed under reduced pressure. Cold water was then added; extraction was done twice with ethyl acetate. Combined organic layers were dried with sodium sulfate. Organic layer was then dried under reduced pressure to yield the final product.

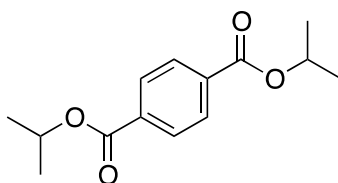
### Spectroscopic data



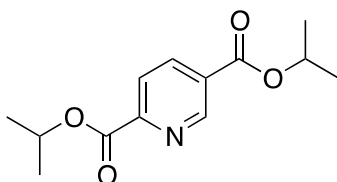
Dimethyl terephthalate (**3**): White solid; IR (Nujol) 1719 ( $\text{O}-\text{C}=\text{O}$ )  $\text{cm}^{-1}$ ;  $^1\text{H}$  NMR ( $\text{CDCl}_3$ , 400 MHz)  $\delta$  8.10 (s, 4H), 3.95 (s, 6H);  $^{13}\text{C}$  NMR ( $\text{CDCl}_3$ , 400 MHz)  $\delta$  166.3, 133.9, 129.6, 52.4; HRMS ESI ( $m/z$ ): found, 195.0647, calcd for  $\text{C}_{10}\text{H}_{11}\text{O}_4$ :  $[\text{M}+\text{H}]^+$ , 195.0657.



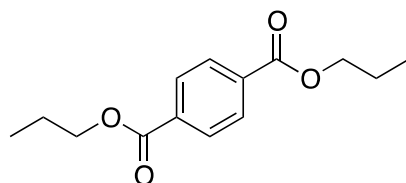
Dimethyl pyridine-2,5-dicarboxylate (**4**): White solid; IR (Nujol) 1717 ( $\text{O}-\text{C}=\text{O}$ )  $\text{cm}^{-1}$ ;  $^1\text{H}$  NMR ( $\text{CDCl}_3$ , 400 MHz)  $\delta$  9.30 (dd, 1H,  $J = 1.98, 0.64$  Hz), 8.43 (dd, 1H,  $J = 8.14, 2.12$  Hz), 8.19 (dd, 1H,  $J = 8.10, 0.68$  Hz), 4.03 (s, 3H), 3.98 (s, 3H);  $^{13}\text{C}$  NMR ( $\text{CDCl}_3$ , 400 MHz)  $\delta$  164.9, 164.8, 150.8, 150.7, 138.3, 128.6, 124.7, 53.2, 52.7; HRMS ESI ( $m/z$ ): found, 196.0605, calcd for  $\text{C}_9\text{H}_{10}\text{NO}_4$ :  $[\text{M}+\text{H}]^+$ , 196.0610.



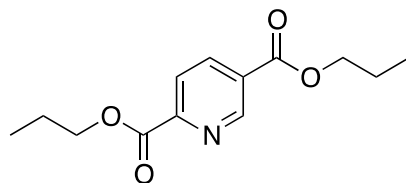
Diisopropyl terephthalate (**5**). White solid: IR (Nujol) 1722 ( $\text{O}-\text{C}=\text{O}$ )  $\text{cm}^{-1}$ ;  $^1\text{H}$  NMR ( $\text{CDCl}_3$ , 400 MHz)  $\delta$  8.08 (s, 4H), 5.29-5.24 (m, 2H), 1.38 (dd, 12H,  $J = 6.20, 3.04$  Hz);  $^{13}\text{C}$  NMR ( $\text{CDCl}_3$ , 400 MHz)  $\delta$  165.4, 134.5, 129.4, 68.9, 21.9; HRMS ESI ( $m/z$ ): found, 251.1274, calcd for  $\text{C}_{14}\text{H}_{19}\text{O}_4$ :  $[\text{M}+\text{H}]^+$ , 251.1283.



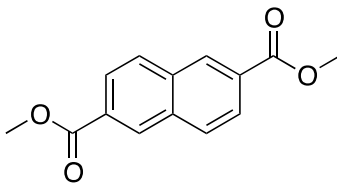
Diisopropyl pyridine-2,5-dicarboxylate (**6**). Pale-yellow solid; IR (Nujol) 1726 (O–C=O)  $\text{cm}^{-1}$ ;  $^1\text{H}$  NMR ( $\text{CDCl}_3$ , 400 MHz) 9.31 (d, 1H,  $J = 1.32$  Hz), 8.39 (dd, 1H,  $J = 8.10, 2.04$  Hz), 8.15 (d, 1H,  $J = 8.16$  Hz), 5.38-5.28 (m, 2H), 1.39 (dd, 12H,  $J = 16.02, 6.28$  Hz);  $^{13}\text{C}$  NMR ( $\text{CDCl}_3$ , 400 MHz)  $\delta$  164.1, 164.0, 151.5, 150.9, 138.0, 129.0, 124.4, 70.1, 69.7, 21.8; HRMS ESI ( $m/z$ ): found, 252.1229, calcd for  $\text{C}_{13}\text{H}_{18}\text{NO}_4$ :  $[\text{M}+\text{H}]^+$ , 252.1236.



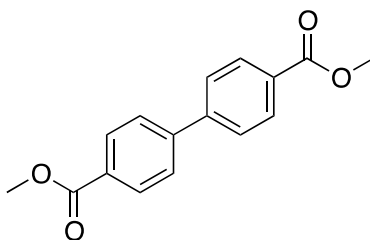
Dipropyl terephthalate (**7**). White solid; IR (Nujol) 1726 (O–C=O)  $\text{cm}^{-1}$ ;  $^1\text{H}$  NMR ( $\text{CDCl}_3$ , 400 MHz)  $\delta$  8.10 (s, 4H), 4.29 (t, 4H,  $J = 6.68$  Hz), 1.85-1.76 (m, 4H), 1.02 (t, 6H,  $J = 7.4$  Hz);  $^{13}\text{C}$  NMR ( $\text{CDCl}_3$ , 400 MHz)  $\delta$  165.9, 134.2, 129.4, 66.9, 22.0, 10.5; HRMS ESI ( $m/z$ ): found, 251.1275, calcd for  $\text{C}_{14}\text{H}_{19}\text{O}_4$ :  $[\text{M}+\text{H}]^+$ , 251.1283.



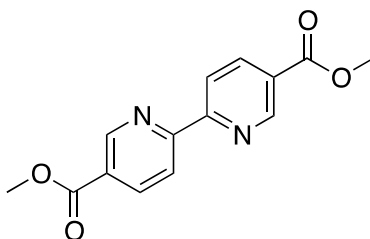
Dipropyl pyridine-2,5-dicarboxylate (**8**). Yellow oil; IR 1730 (O–C=O)  $\text{cm}^{-1}$ ;  $^1\text{H}$  NMR ( $\text{CDCl}_3$ , 400 MHz)  $\delta$  9.28 (s, 1H), 8.38 (dd, 1H,  $J = 8.10, 2.04$  Hz), 8.14 (d, 1H,  $J = 8.12$  Hz), 4.35 (t, 2H,  $J = 6.84$  Hz), 4.29 (t, 2H,  $J = 6.64$  Hz), 1.85-1.76 (m, 4H), 1.02-0.98 (m, 6H);  $^{13}\text{C}$  NMR ( $\text{CDCl}_3$ , 400 MHz)  $\delta$  164.5, 164.4, 151.2, 150.8, 138.1, 128.7, 124.5, 67.8, 67.4, 22.0, 10.4, 10.3; HRMS ESI ( $m/z$ ): found, 252.1244, calcd for  $\text{C}_{13}\text{H}_{18}\text{NO}_4$ :  $[\text{M}+\text{H}]^+$ , 252.1236.



Dimethyl naphthalene-2,6-dicarboxylate (**9**). Pale-yellow solid; mp: 190-192  $^\circ\text{C}$ ; IR (Nujol) 1713 (O–C=O)  $\text{cm}^{-1}$ ;  $^1\text{H}$  NMR ( $\text{CDCl}_3$ , 400 MHz)  $\delta$  8.63 (s, 2H), 8.11 (dd, 2H,  $J = 8.58, 1.16$  Hz), 7.99 (d, 2H,  $J = 8.56$  Hz), 4.00 (s, 3H);  $^{13}\text{C}$  NMR ( $\text{CDCl}_3$ , 400 MHz)  $\delta$  166.8, 134.6, 130.6, 129.6, 126.0, 52.4; HRMS ESI ( $m/z$ ): found, 245.0821, calcd for  $\text{C}_{14}\text{H}_{12}\text{O}_4$ :  $[\text{M}+\text{H}]^+$ , 245.0814.



Dimethyl biphenyl-4,4'-dicarboxylate (**10**): White solid; IR (Nujol) 1719 (O–C=O)  $\text{cm}^{-1}$ ;  $^1\text{H}$  NMR ( $\text{CDCl}_3$ , 400 MHz)  $\delta$  8.13 (d,  $J = 8.12$  Hz, 4H), 7.79 (d,  $J = 8.12$  Hz, 4H), 3.95 (s, 6H);  $^{13}\text{C}$  NMR ( $\text{CDCl}_3$ , 400 MHz)  $\delta$  166.8, 144.4, 130.2, 129.7, 127.2, 52.2; HRMS ESI ( $m/z$ ): found, 271.0974, calcd for  $\text{C}_{16}\text{H}_{15}\text{O}_4$ :  $[\text{M}+\text{H}]^+$ , 271.0970.



Dimethyl [2,2'-bipyridine]-5,5'-dicarboxylate (**11**): White solid; mp: 266-270  $^\circ\text{C}$ ; IR (Nujol) 1728 (O–C=O)  $\text{cm}^{-1}$ ;  $^1\text{H}$  NMR ( $\text{CDCl}_3$ , 400 MHz)  $\delta$  9.32 (s, 2H), 8.61 (d,  $J = 8.28$  Hz, 2H), 8.45 (dd, 2H,  $J = 8.26, 2.04$  Hz), 4.02 (s, 6H);  $^{13}\text{C}$  NMR ( $\text{CDCl}_3$ , 400 MHz)  $\delta$  165.6, 158.4, 150.6, 138.1, 126.3, 121.3, 52.5; HRMS ESI ( $m/z$ ): found, 273.0866, calcd for  $\text{C}_{14}\text{H}_{13}\text{N}_2\text{O}_4$ :  $[\text{M}+\text{H}]^+$ , 273.0875.

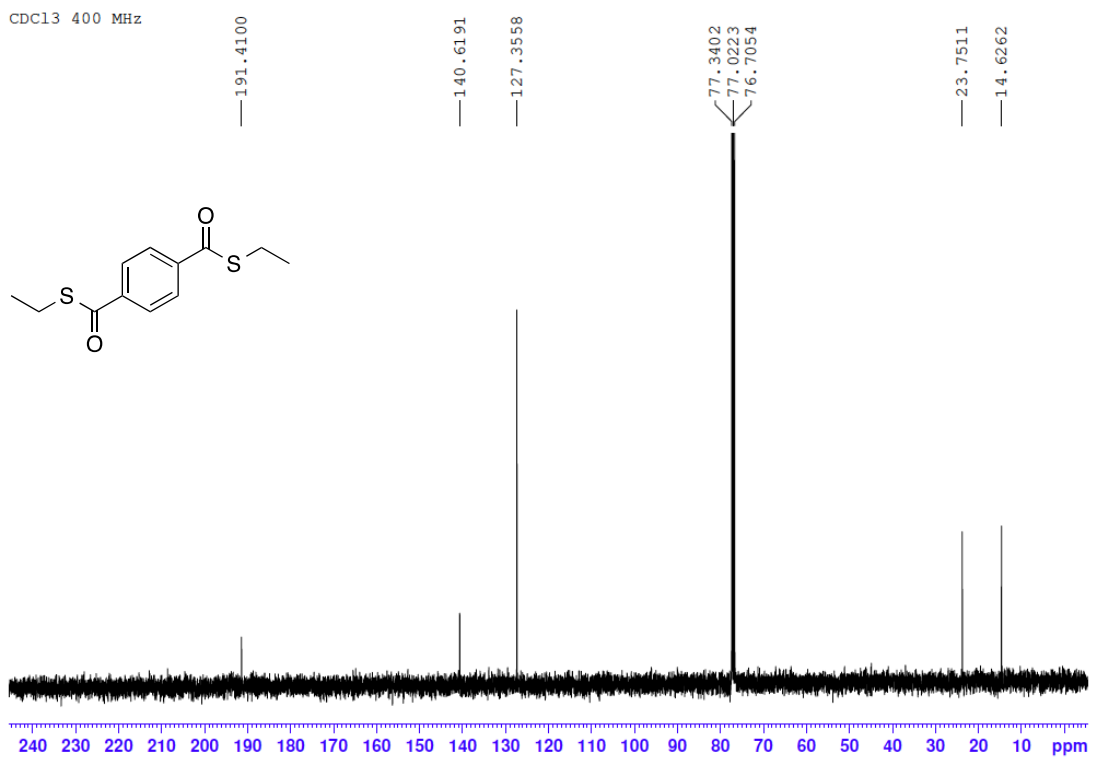
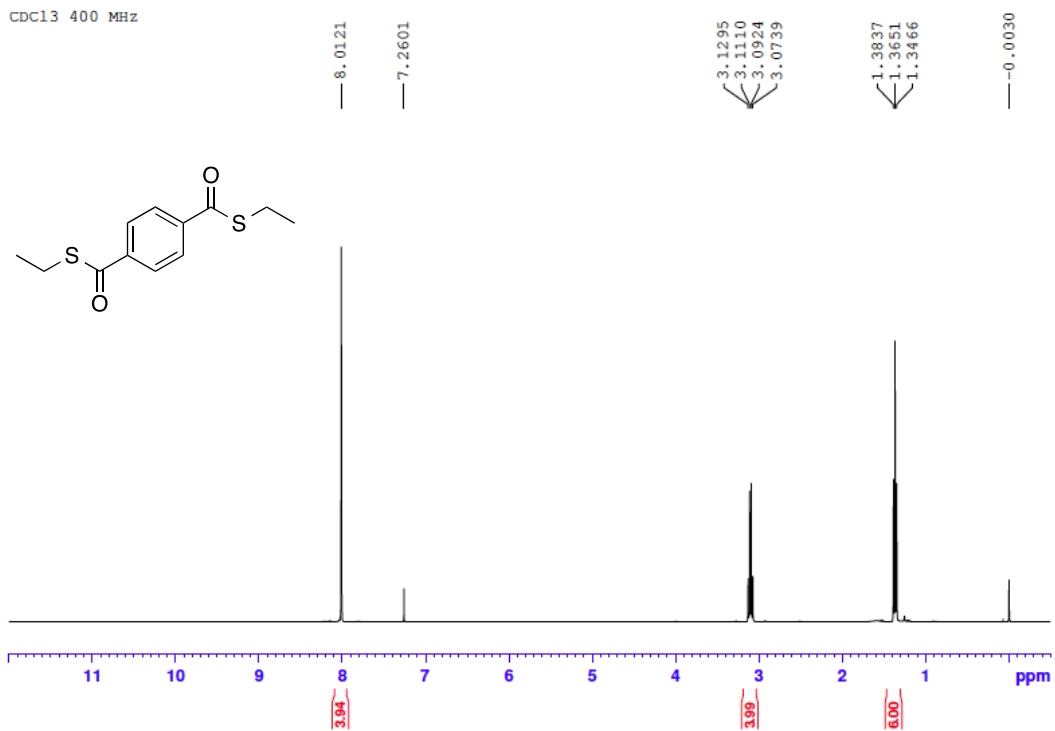


**Figure S1.**  $^1\text{H}$  and  $^{13}\text{C}$  NMR spectra of *S,S*-diethyl benzene-1,4-bis(carbothioate) (compound **1**).

CDC13 400 MHz

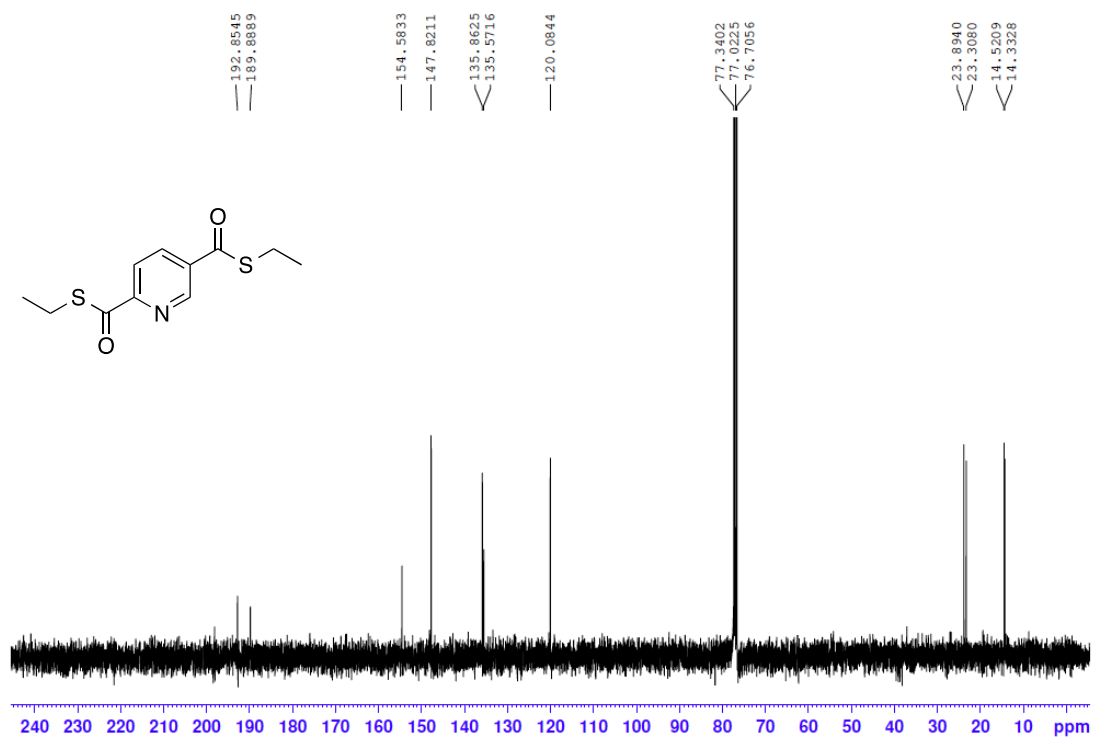
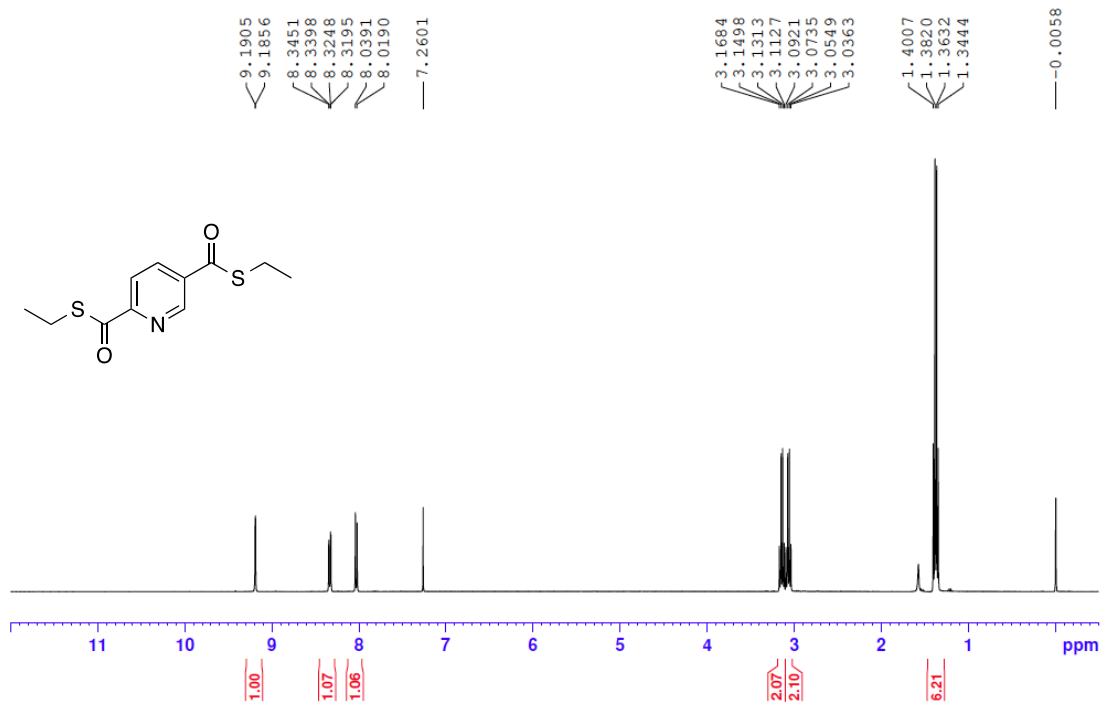


**Figure S2.** <sup>1</sup>H and <sup>13</sup>C NMR spectra of *S,S*-diethyl pyridine-2,5-bis(carbothioate) (compound 2).

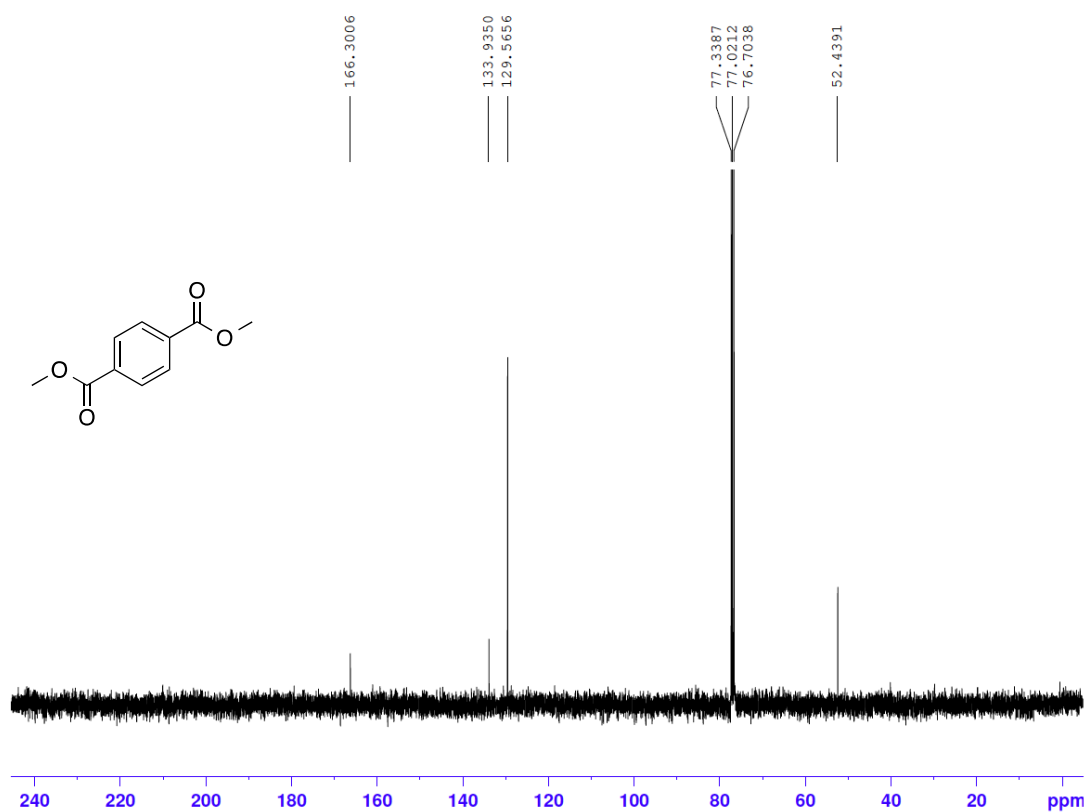
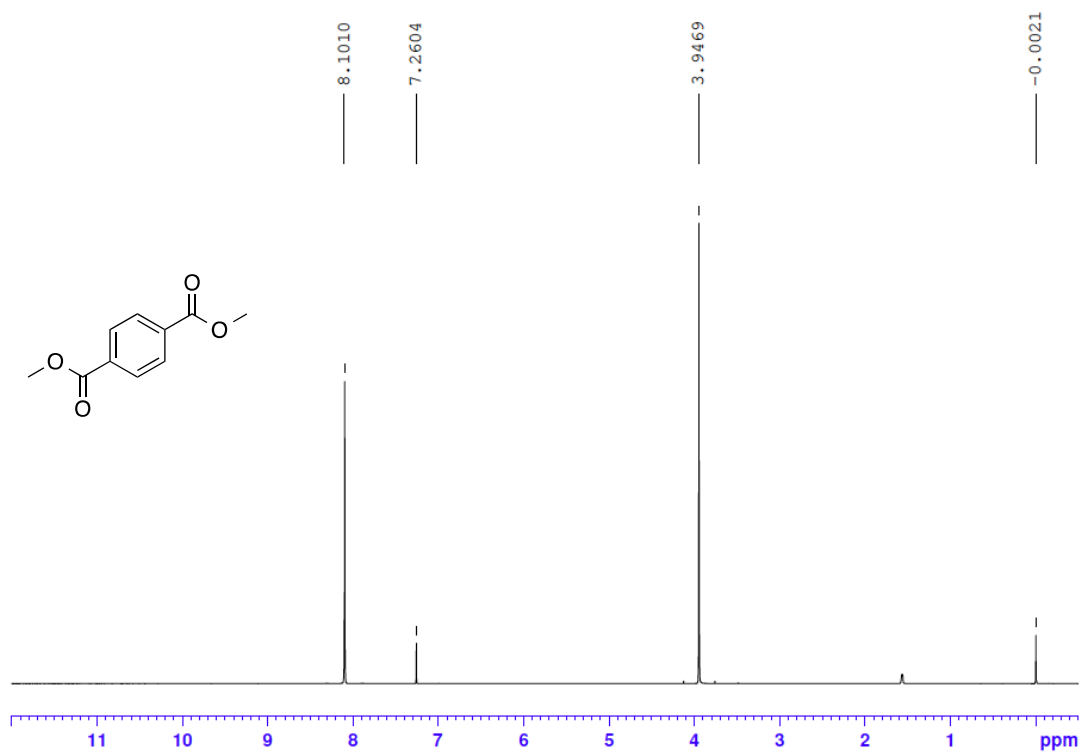


**Figure S3.**  $^1\text{H}$  and  $^{13}\text{C}$  NMR spectra of dimethyl terephthalate (compound **3**).

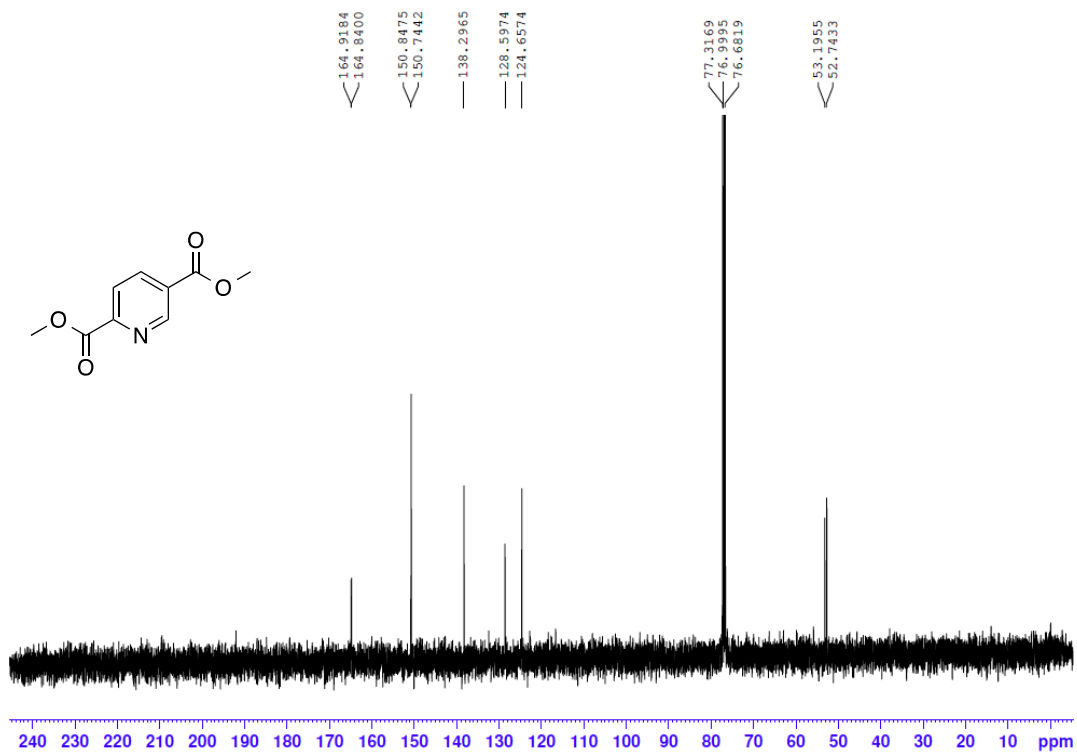
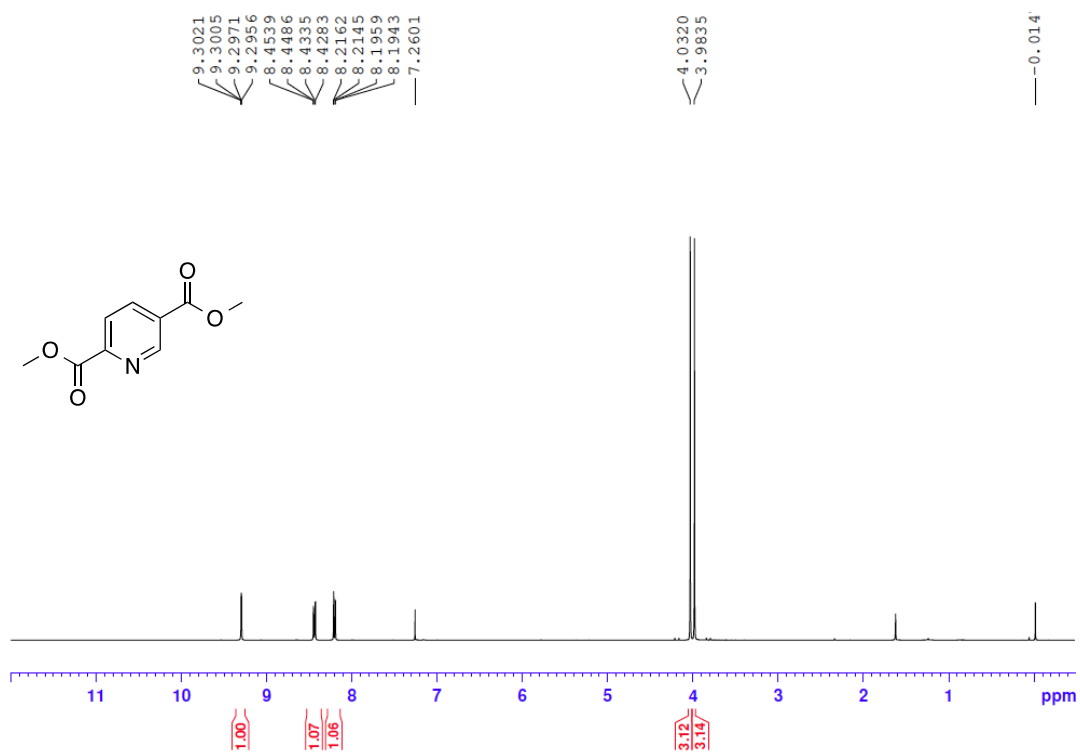


**Figure S4.** <sup>1</sup>H and <sup>13</sup>C NMR spectra of dimethyl pyridine-2,5-dicarboxylate (compound 4).

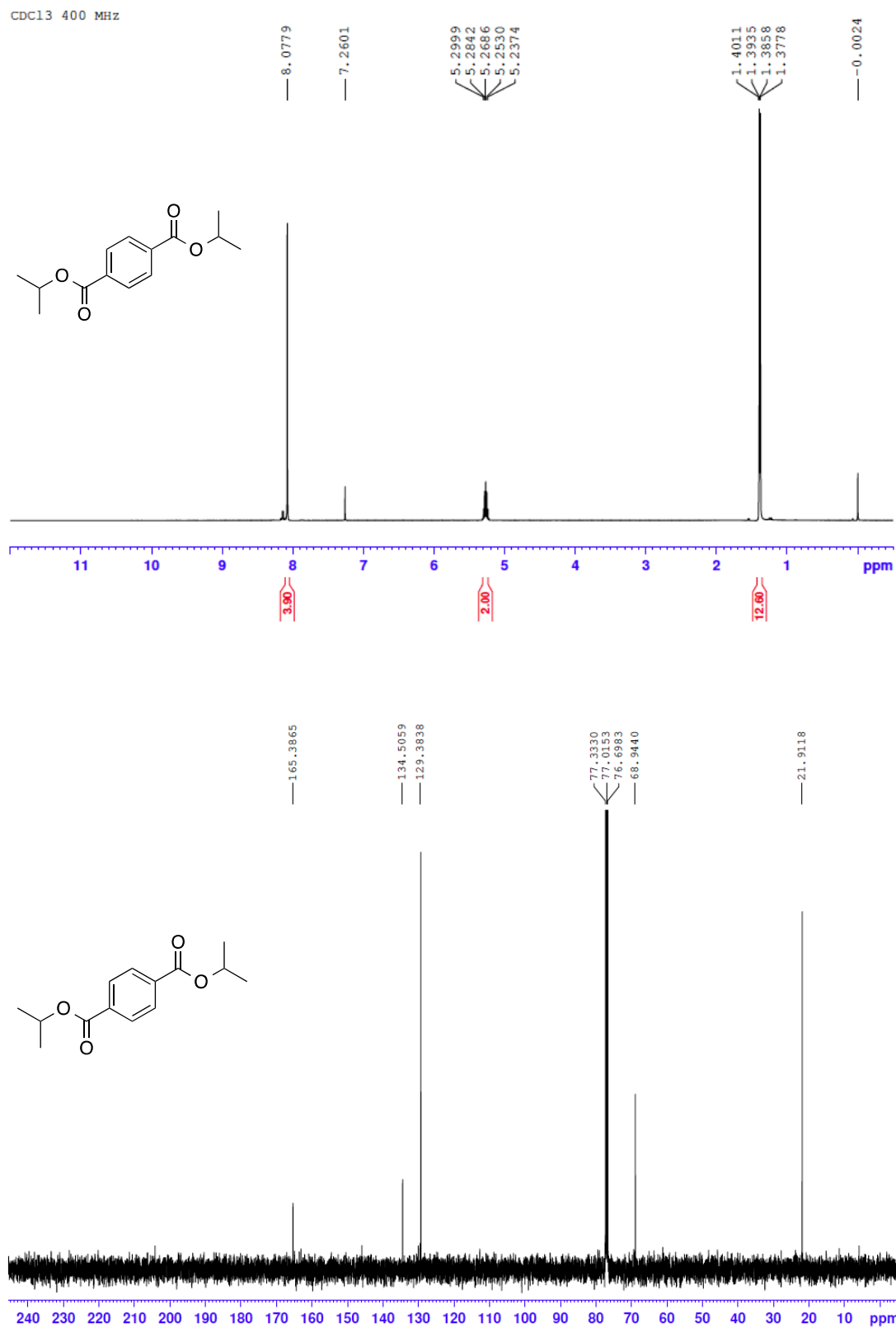


**Figure S5.** <sup>1</sup>H and <sup>13</sup>C NMR spectra of diisopropyl terephthalate (compound **5**).

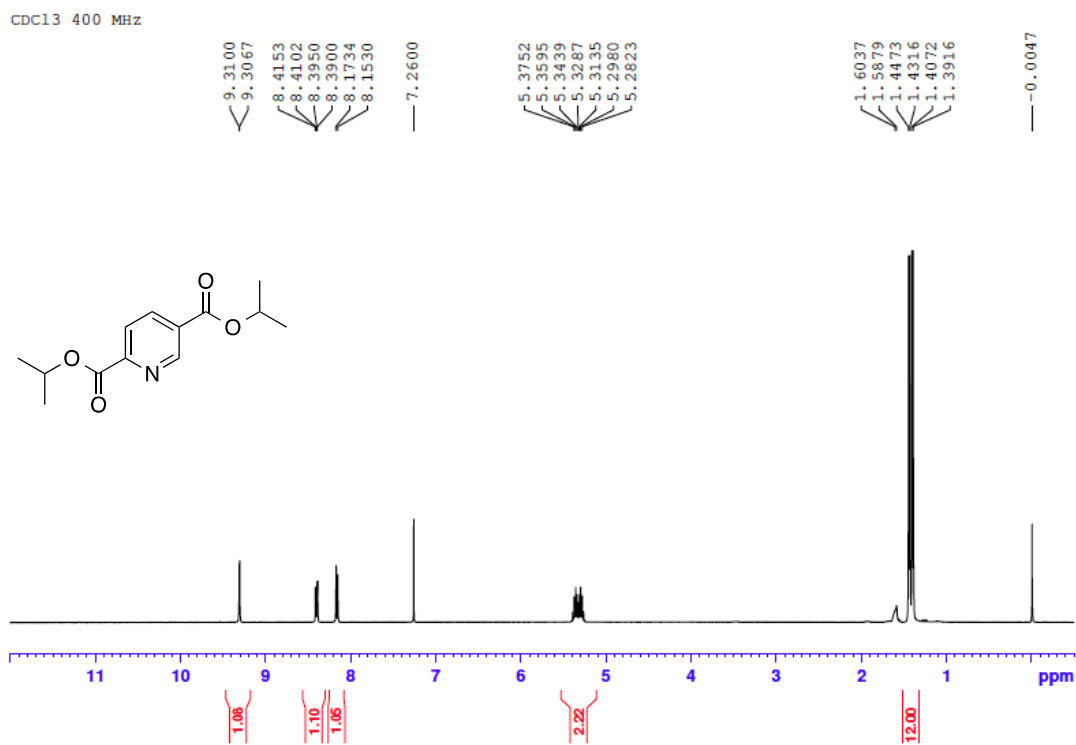
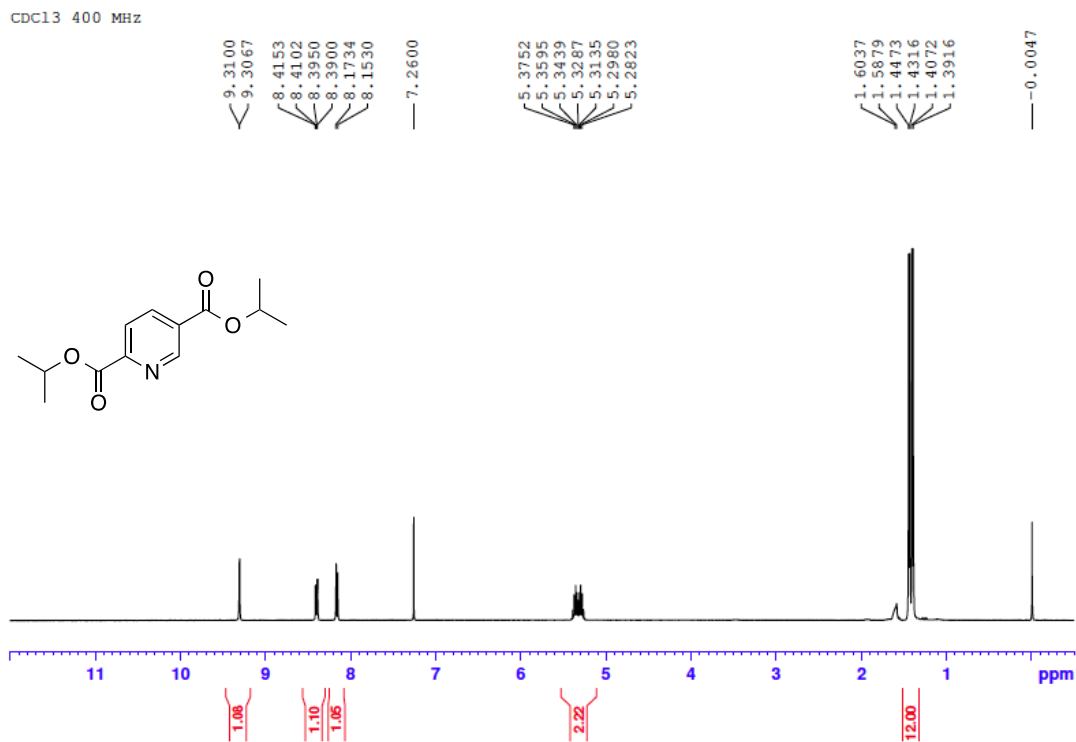


**Figure S6.**  $^1\text{H}$  and  $^{13}\text{C}$  NMR spectra of diisopropyl pyridine-2,5-dicarboxylate (compound 6).

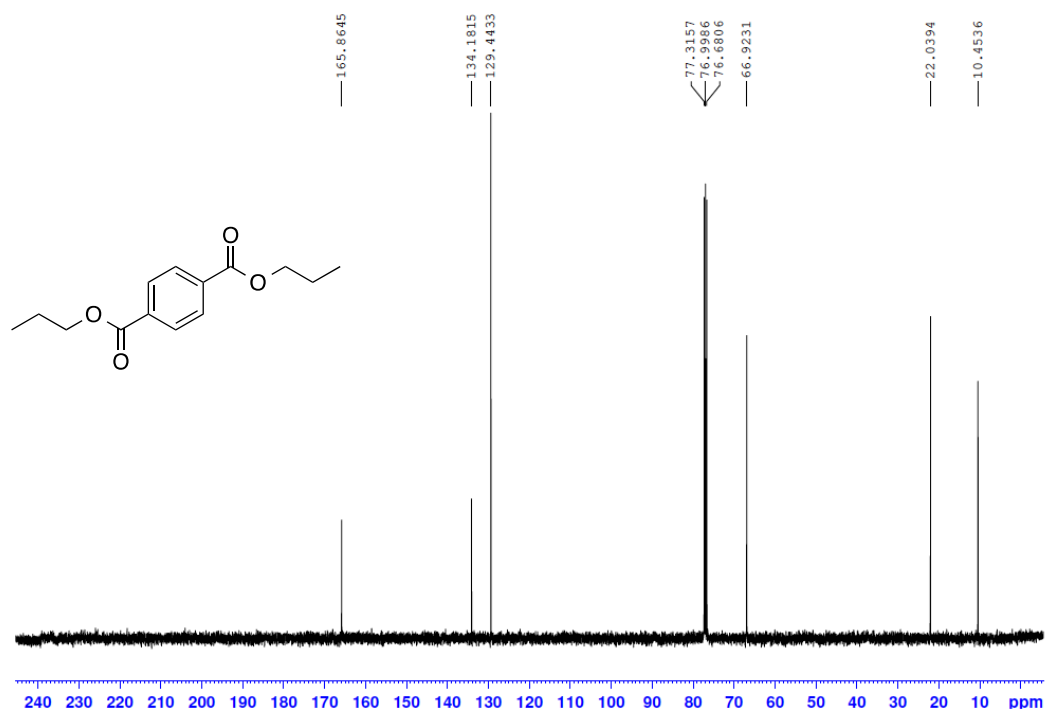
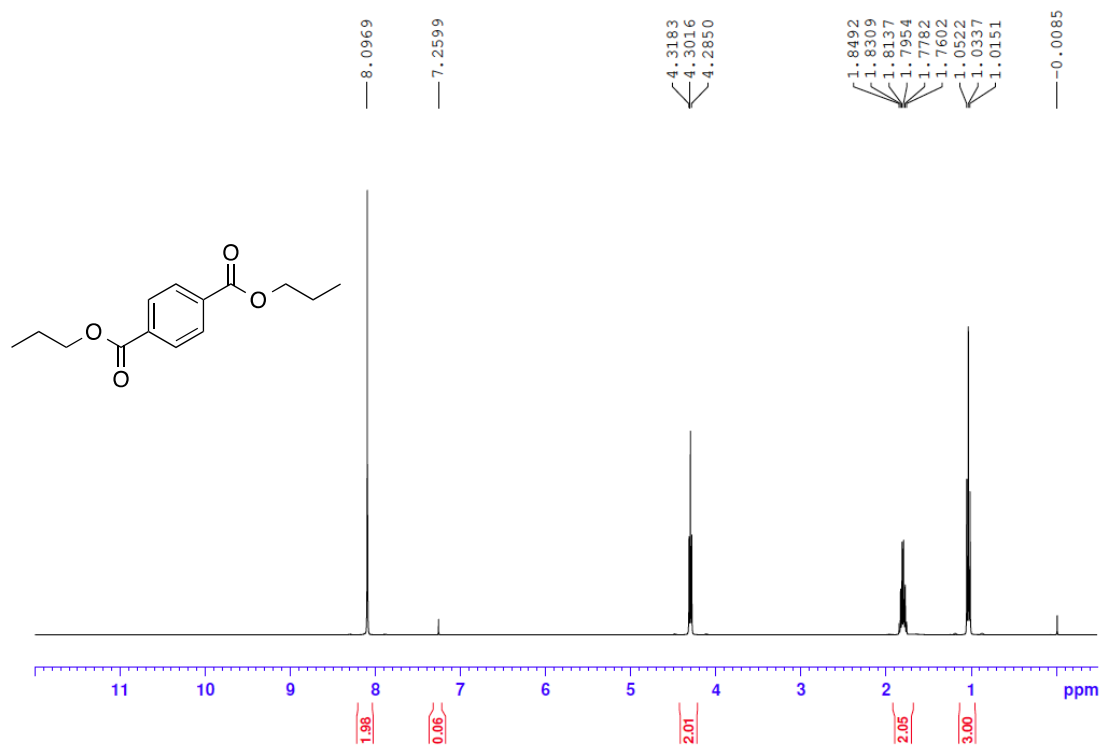


**Figure S7.** <sup>1</sup>H and <sup>13</sup>C NMR spectra of dipropyl terephthalate (compound 7).

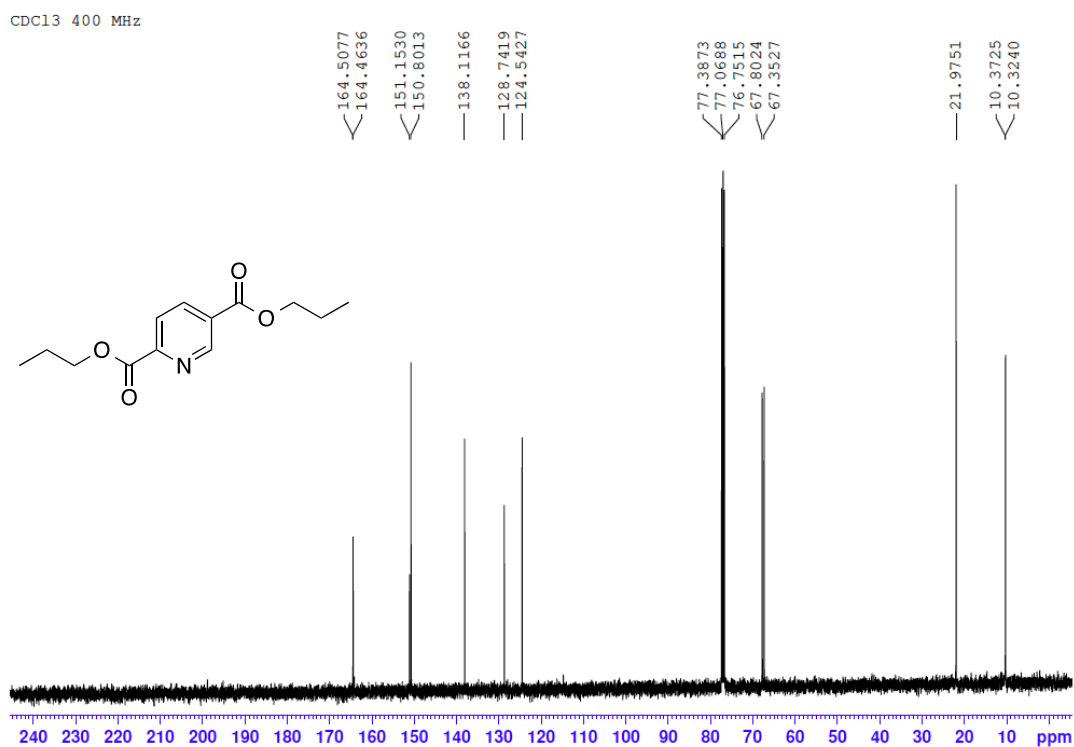
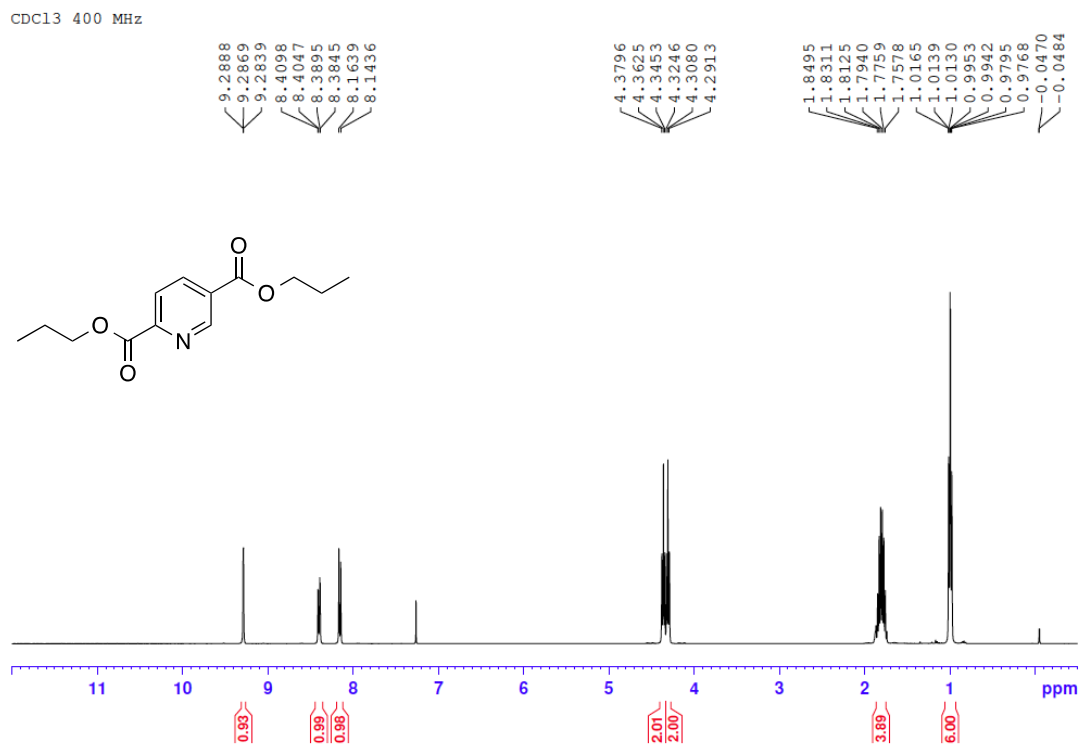


**Figure S8.**  $^1\text{H}$  and  $^{13}\text{C}$  NMR spectra of dipropyl pyridine-2,5-dicarboxylate (compound **8**).

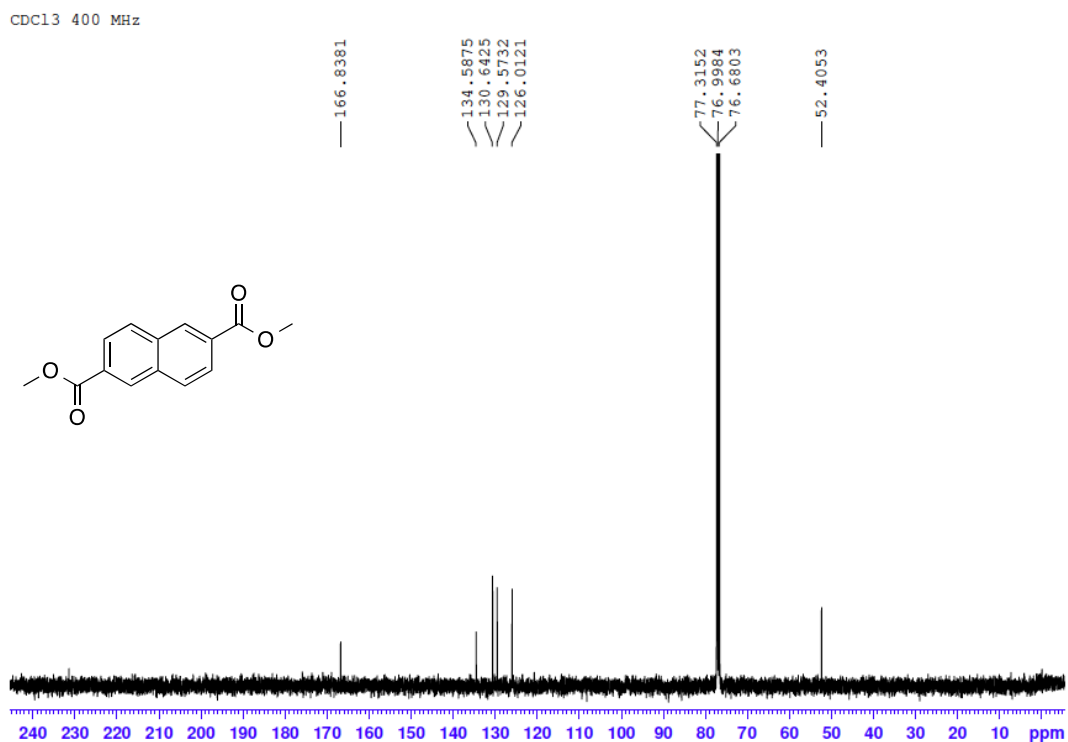
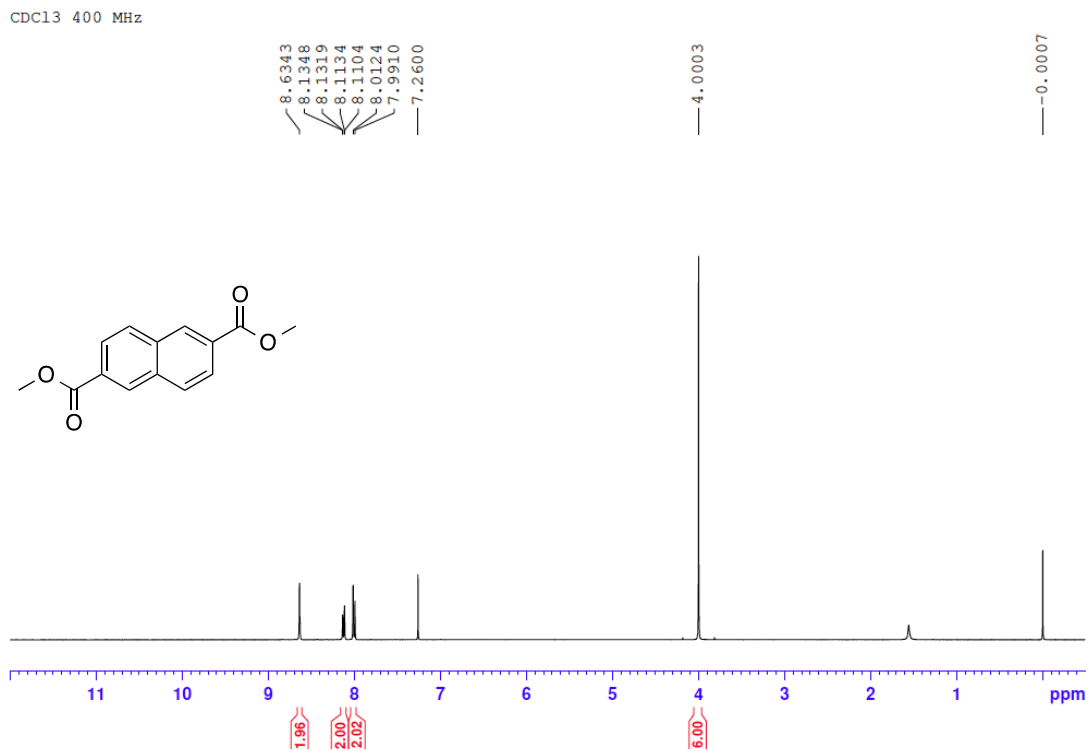


**Figure S9.** <sup>1</sup>H and <sup>13</sup>C NMR spectra of dimethyl naphthalene-2,6-dicarboxylate (compound **9**).

CDC13 400 MHz

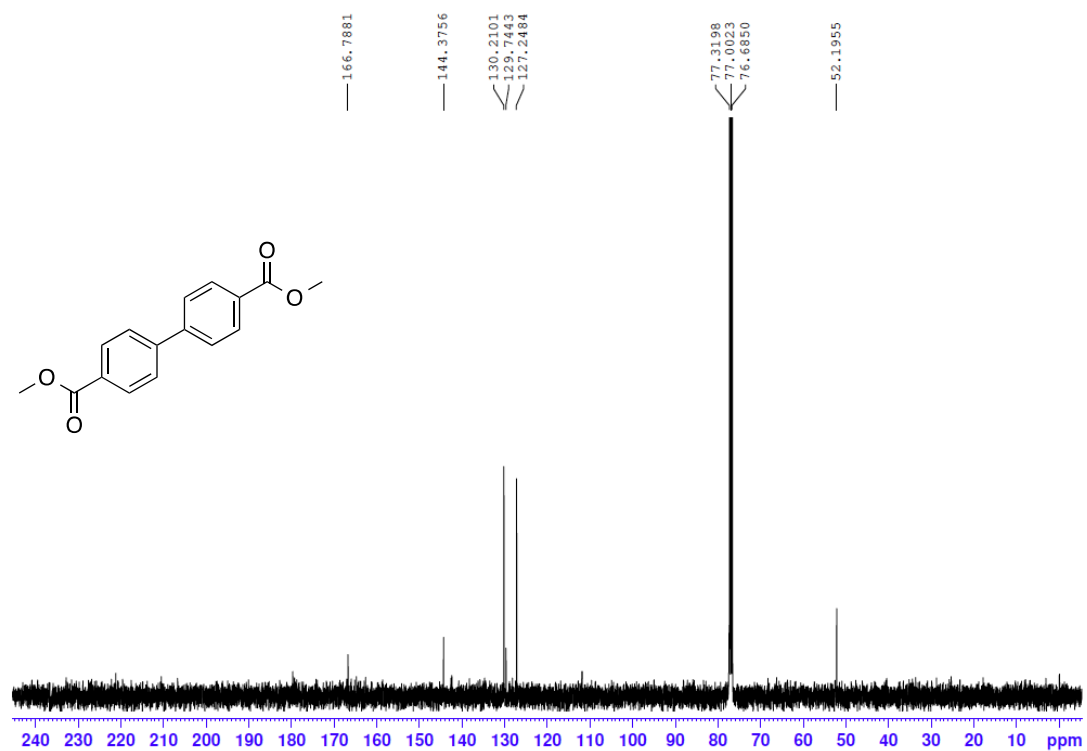
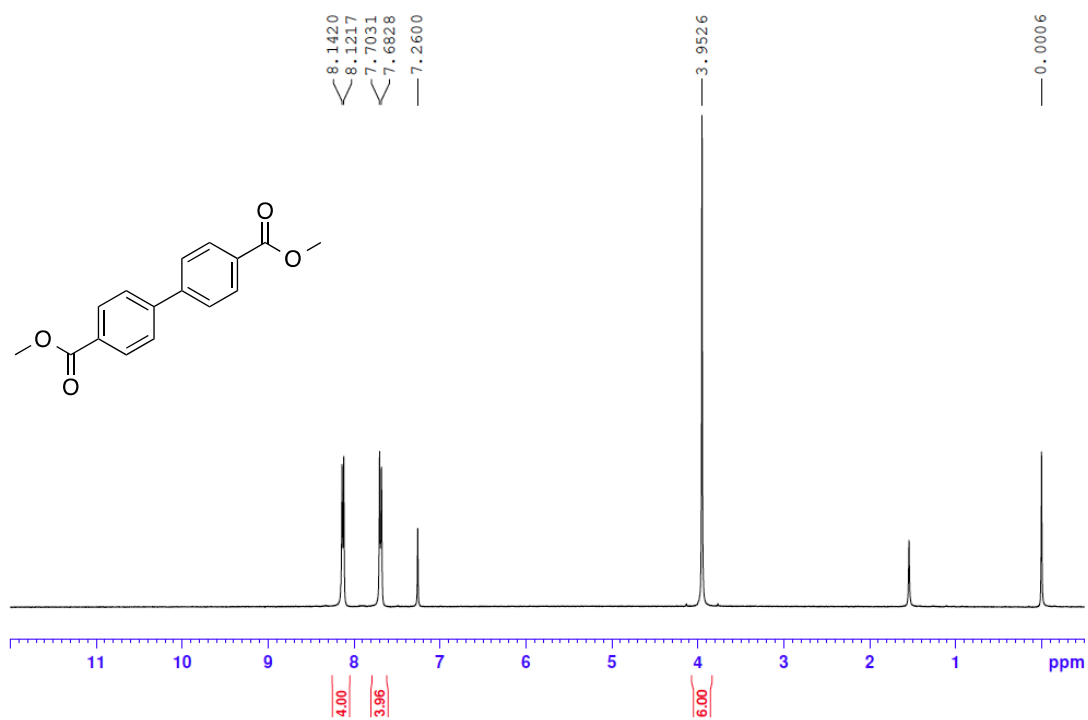


**Figure S10.**  $^1\text{H}$  and  $^{13}\text{C}$  NMR spectra of dimethyl biphenyl-4,4'-dicarboxylate (compound 10).

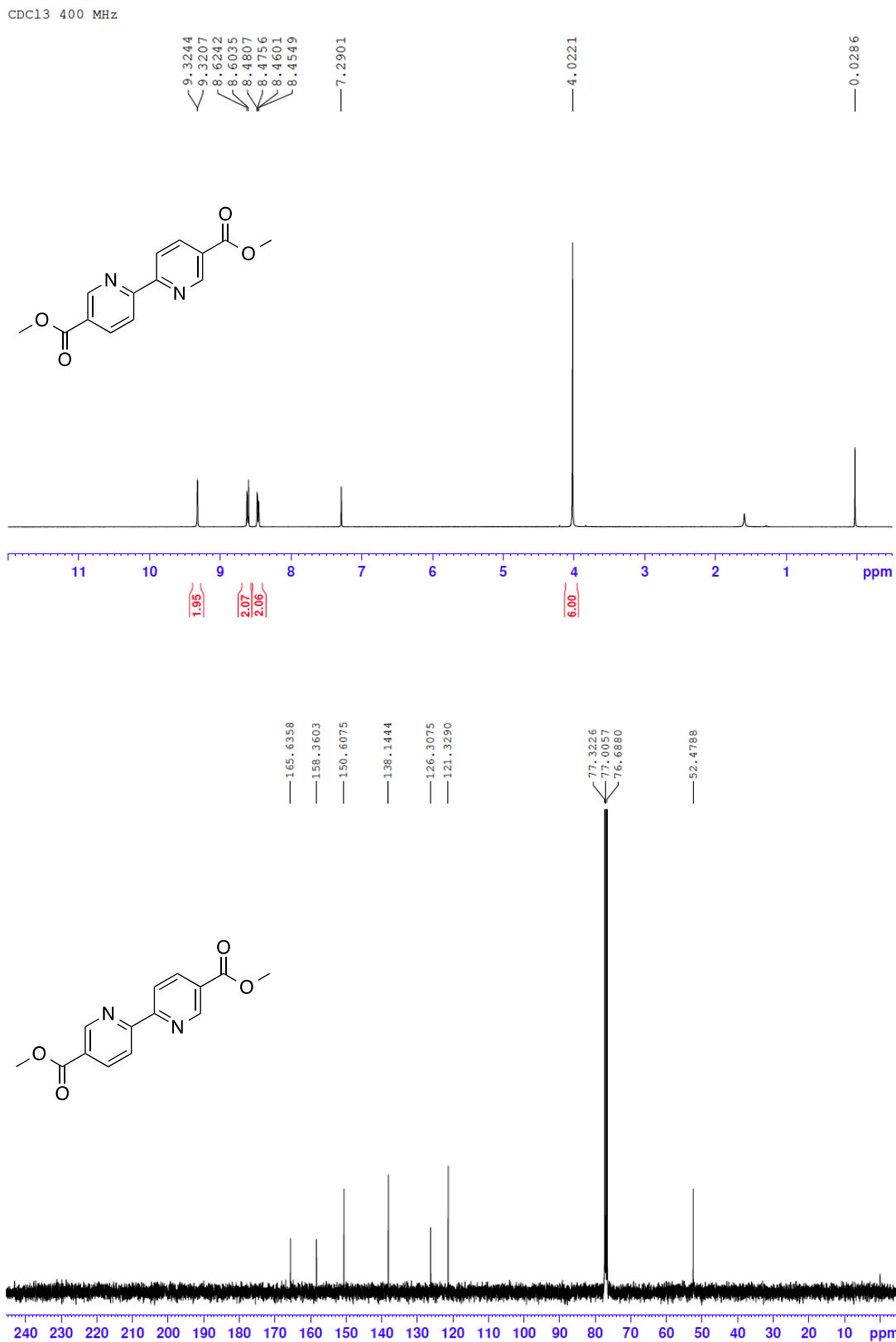


**Figure S11.** <sup>1</sup>H and <sup>13</sup>C NMR spectra of dimethyl [2,2'-bipyridine]-5,5'-dicarboxylate (compound **11**).

**Figure S12.** Cyclic voltammograms of compound **1** at 20 °C and -30 °C.

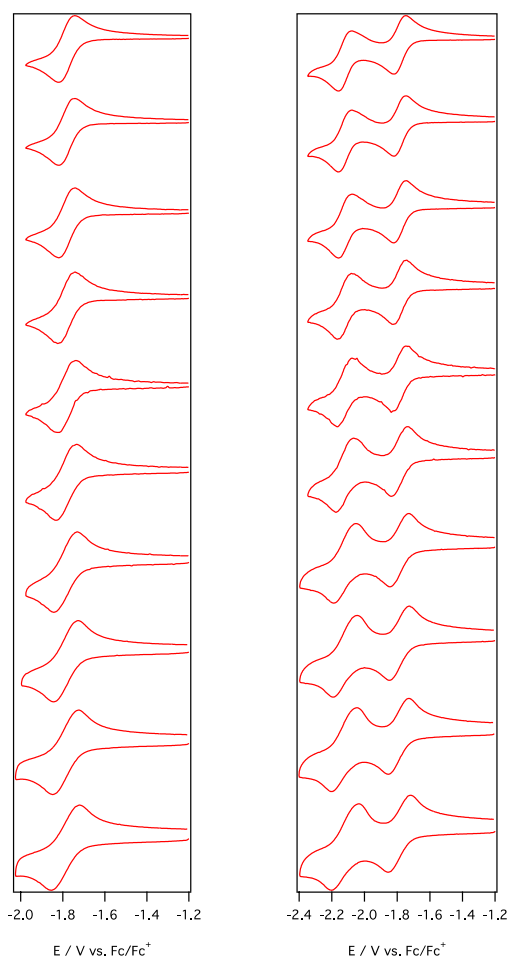


**Figure S12a:** Cyclic voltammograms of **1** at 20 °C. Scan rates ( $\nu$ ) from 0.1 V s<sup>-1</sup>, 0.2 V s<sup>-1</sup>, 0.5 V s<sup>-1</sup>, 1.0 V s<sup>-1</sup>, 2.0 V s<sup>-1</sup>, 5 V s<sup>-1</sup>, 10 V s<sup>-1</sup>, 12 V s<sup>-1</sup>, 15 V s<sup>-1</sup> and 20 V s<sup>-1</sup> (top to bottom) obtained at a glassy carbon electrode in CH<sub>3</sub>CN (0.2 M Bu<sub>4</sub>NPF<sub>6</sub>) for the 1-electron reduction (left) and 2-electron reduction (right) of *ca.* 2 mM analyte. Current data were scaled by multiplying by  $\nu^{0.5}$ .

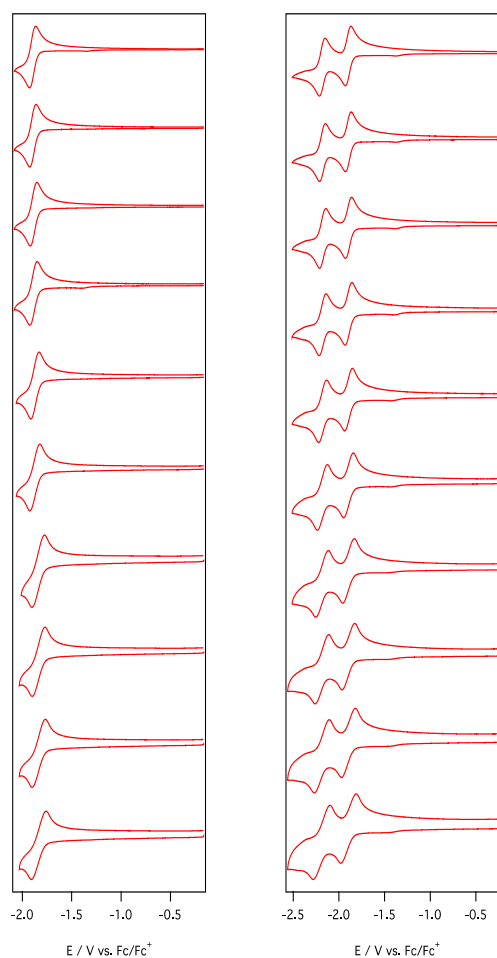


**Figure S12b:** Cyclic voltammograms of **1** at -30 °C. Scan rates ( $\nu$ ) from 0.1 V s<sup>-1</sup>, 0.2 V s<sup>-1</sup>, 0.5 V s<sup>-1</sup>, 1.0 V s<sup>-1</sup>, 2.0 V s<sup>-1</sup>, 5 V s<sup>-1</sup>, 10 V s<sup>-1</sup>, 12 V s<sup>-1</sup>, 15 V s<sup>-1</sup> and 20 V s<sup>-1</sup> (top to bottom) obtained at a glassy carbon electrode in CH<sub>3</sub>CN (0.2 M Bu<sub>4</sub>NPF<sub>6</sub>) for the 1-electron reduction (left) and 2-electron reduction (right) of *ca.* 2 mM analyte. Current data were scaled by multiplying by  $\nu^{0.5}$ .

**Figure S13.** Cyclic voltammograms of compound **2** at 20 °C and -30 °C.

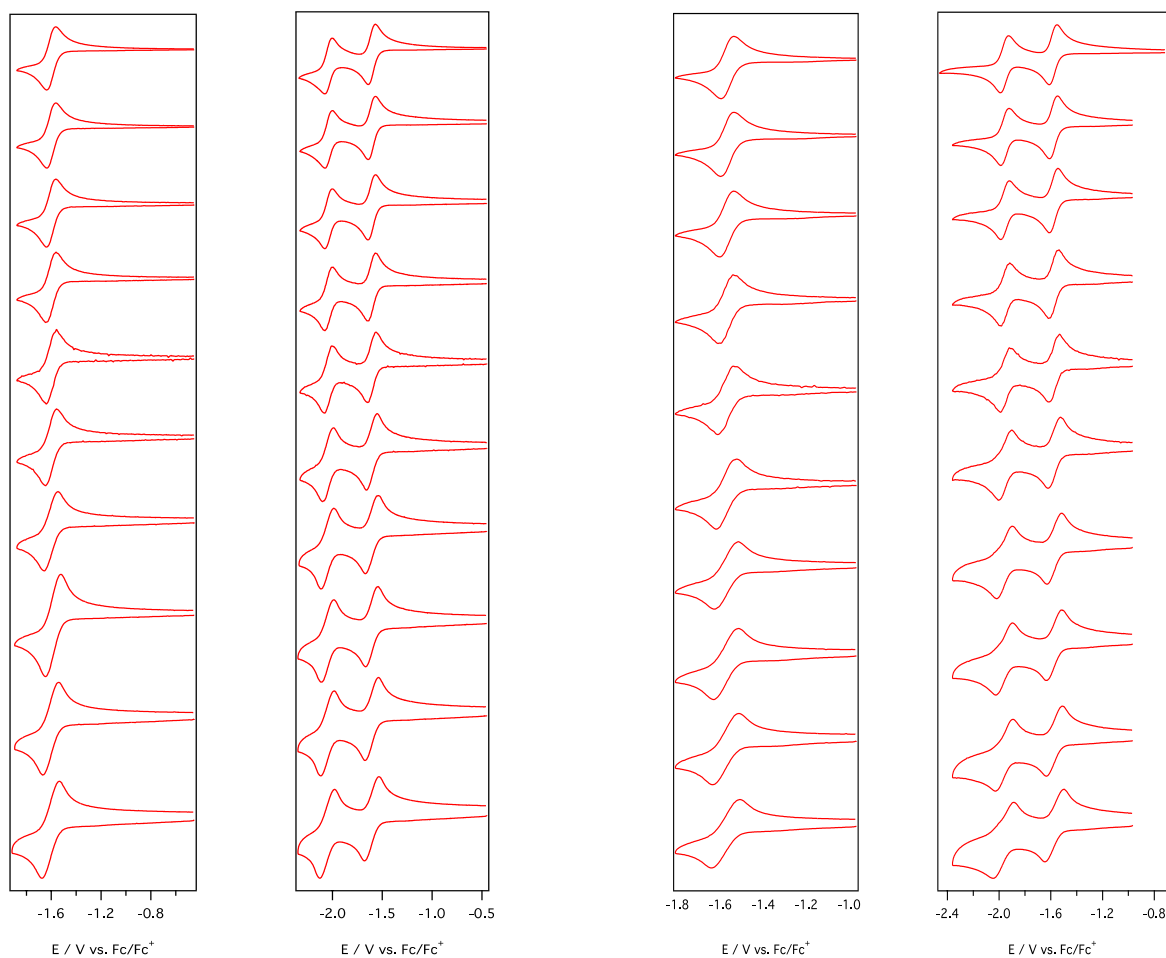


**Figure S13a:** Cyclic voltammograms of **2** at 20 °C. Scan rates ( $\nu$ ) from 0.1 V s<sup>-1</sup>, 0.2 V s<sup>-1</sup>, 0.5 V s<sup>-1</sup>, 1.0 V s<sup>-1</sup>, 2.0 V s<sup>-1</sup>, 5 V s<sup>-1</sup>, 10 V s<sup>-1</sup>, 12 V s<sup>-1</sup>, 15 V s<sup>-1</sup> and 20 V s<sup>-1</sup> (top to bottom) obtained at a glassy carbon electrode in CH<sub>3</sub>CN (0.2 M Bu<sub>4</sub>NPF<sub>6</sub>) for the 1-electron reduction (left) and 2-electron reduction (right) of *ca.* 2 mM analyte. Current data were scaled by multiplying by  $\nu^{0.5}$ .

**Figure S13b:** Cyclic voltammograms of **2** at -30 °C. Scan rates ( $\nu$ ) from 0.1 V s<sup>-1</sup>, 0.2 V s<sup>-1</sup>, 0.5 V s<sup>-1</sup>, 1.0 V s<sup>-1</sup>, 2.0 V s<sup>-1</sup>, 5 V s<sup>-1</sup>, 10 V s<sup>-1</sup>, 12 V s<sup>-1</sup>, 15 V s<sup>-1</sup> and 20 V s<sup>-1</sup> (top to bottom) obtained at a glassy carbon electrode in CH<sub>3</sub>CN (0.2 M Bu<sub>4</sub>NPF<sub>6</sub>) for the 1-electron reduction (left) and 2-electron reduction (right) of *ca.* 2 mM analyte. Current data were scaled by multiplying by  $\nu^{0.5}$ .

**Figure S14.** Cyclic voltammograms of compound **3** at 20 °C and -30 °C.

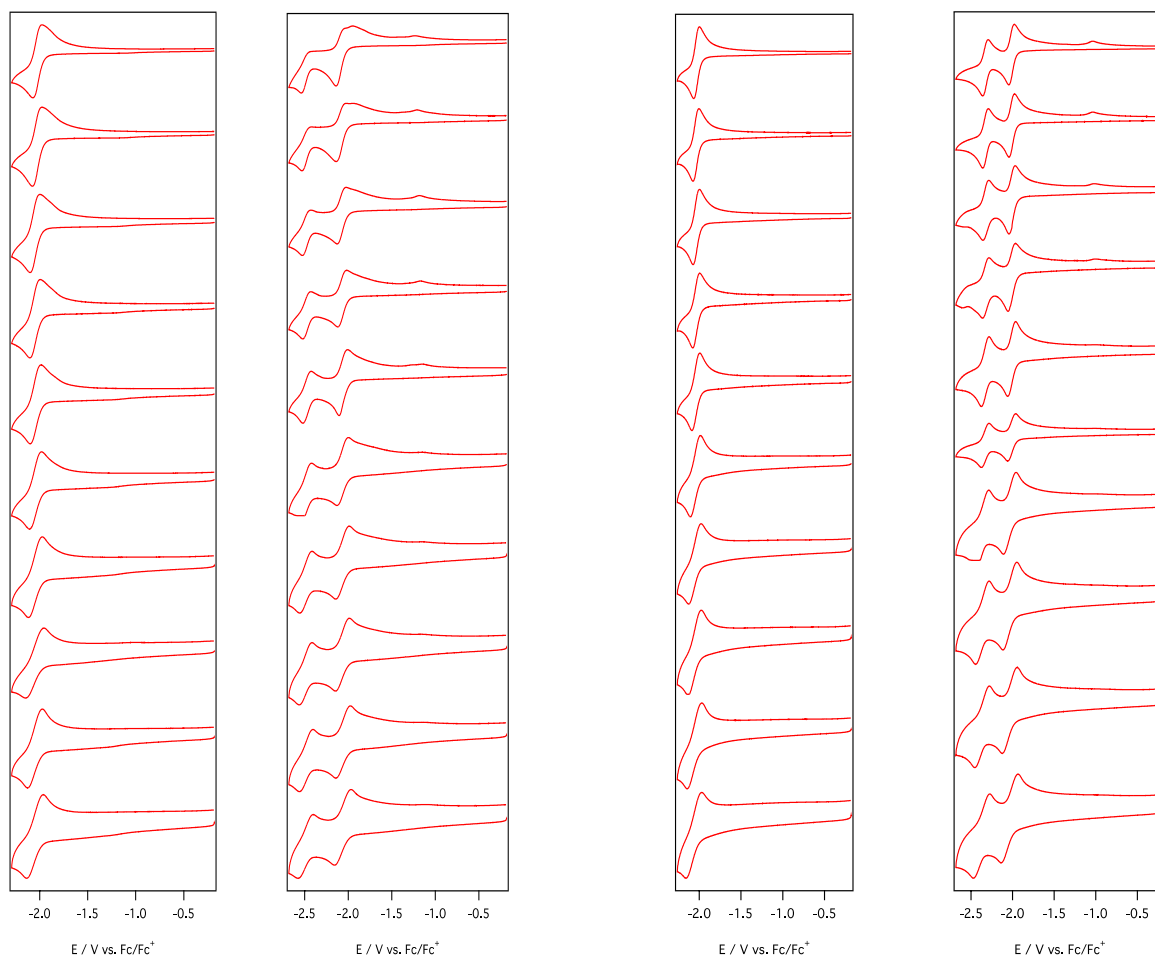


**Figure S14a:** Cyclic voltammograms of **3** at 20 °C. Scan rates ( $\nu$ ) from 0.1 V s<sup>-1</sup>, 0.2 V s<sup>-1</sup>, 0.5 V s<sup>-1</sup>, 1.0 V s<sup>-1</sup>, 2.0 V s<sup>-1</sup>, 5 V s<sup>-1</sup>, 10 V s<sup>-1</sup>, 12 V s<sup>-1</sup>, 15 V s<sup>-1</sup> and 20 V s<sup>-1</sup> (top to bottom) obtained at a glassy carbon electrode in CH<sub>3</sub>CN (0.2 M Bu<sub>4</sub>NPF<sub>6</sub>) for the 1-electron reduction (left) and 2-electron reduction (right) of *ca.* 2 mM analyte. Current data were scaled by multiplying by  $\nu^{0.5}$ .

**Figure S14b:** Cyclic voltammograms of **3** at -30 °C. Scan rates ( $\nu$ ) from 0.1 V s<sup>-1</sup>, 0.2 V s<sup>-1</sup>, 0.5 V s<sup>-1</sup>, 1.0 V s<sup>-1</sup>, 2.0 V s<sup>-1</sup>, 5 V s<sup>-1</sup>, 10 V s<sup>-1</sup>, 12 V s<sup>-1</sup>, 15 V s<sup>-1</sup> and 20 V s<sup>-1</sup> (top to bottom) obtained at a glassy carbon electrode in CH<sub>3</sub>CN (0.2 M Bu<sub>4</sub>NPF<sub>6</sub>) for the 1-electron reduction (left) and 2-electron reduction (right) of *ca.* 2 mM analyte. Current data were scaled by multiplying by  $\nu^{0.5}$ .

**Figure S15.** Cyclic voltammograms of compound **4** at 20 °C and -30 °C.

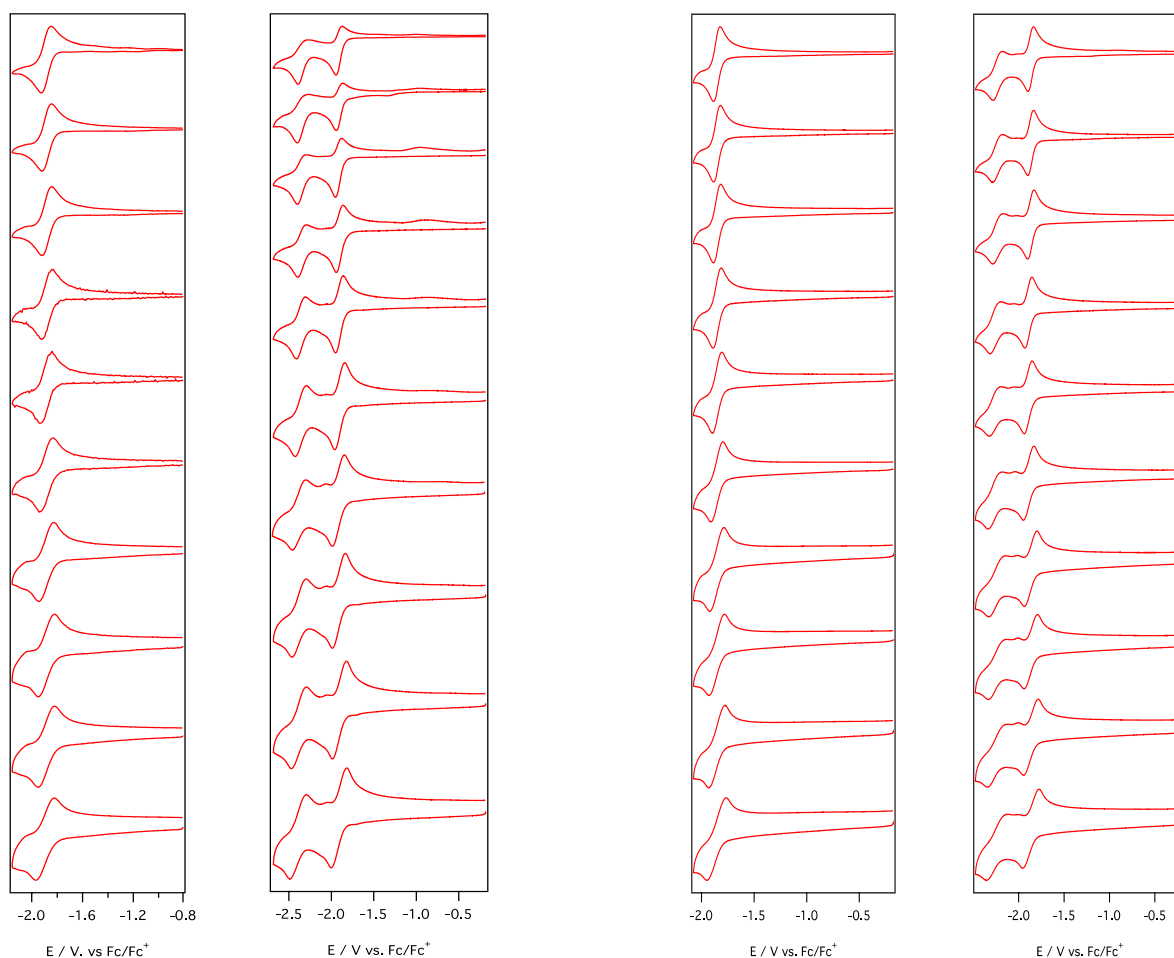


**Figure S15a:** Cyclic voltammograms of **4** at 20 °C. Scan rates ( $\nu$ ) from 0.1 V s<sup>-1</sup>, 0.2 V s<sup>-1</sup>, 0.5 V s<sup>-1</sup>, 1.0 V s<sup>-1</sup>, 2.0 V s<sup>-1</sup>, 5 V s<sup>-1</sup>, 10 V s<sup>-1</sup>, 12 V s<sup>-1</sup>, 15 V s<sup>-1</sup> and 20 V s<sup>-1</sup> (top to bottom) obtained at a glassy carbon electrode in CH<sub>3</sub>CN (0.2 M Bu<sub>4</sub>NPF<sub>6</sub>) for the 1-electron reduction (left) and 2-electron reduction (right) of *ca.* 2 mM analyte. Current data were scaled by multiplying by  $\nu^{-0.5}$ .

**Figure S15b:** Cyclic voltammograms of **4** at -30 °C. Scan rates ( $\nu$ ) from 0.1 V s<sup>-1</sup>, 0.2 V s<sup>-1</sup>, 0.5 V s<sup>-1</sup>, 1.0 V s<sup>-1</sup>, 2.0 V s<sup>-1</sup>, 5 V s<sup>-1</sup>, 10 V s<sup>-1</sup>, 12 V s<sup>-1</sup>, 15 V s<sup>-1</sup> and 20 V s<sup>-1</sup> (top to bottom) obtained at a glassy carbon electrode in CH<sub>3</sub>CN (0.2 M Bu<sub>4</sub>NPF<sub>6</sub>) for the 1-electron reduction (left) and 2-electron reduction (right) of *ca.* 2 mM analyte. Current data were scaled by multiplying by  $\nu^{-0.5}$ .

**Figure S16.** Cyclic voltammograms of compound **5** at 20 °C and -30 °C.

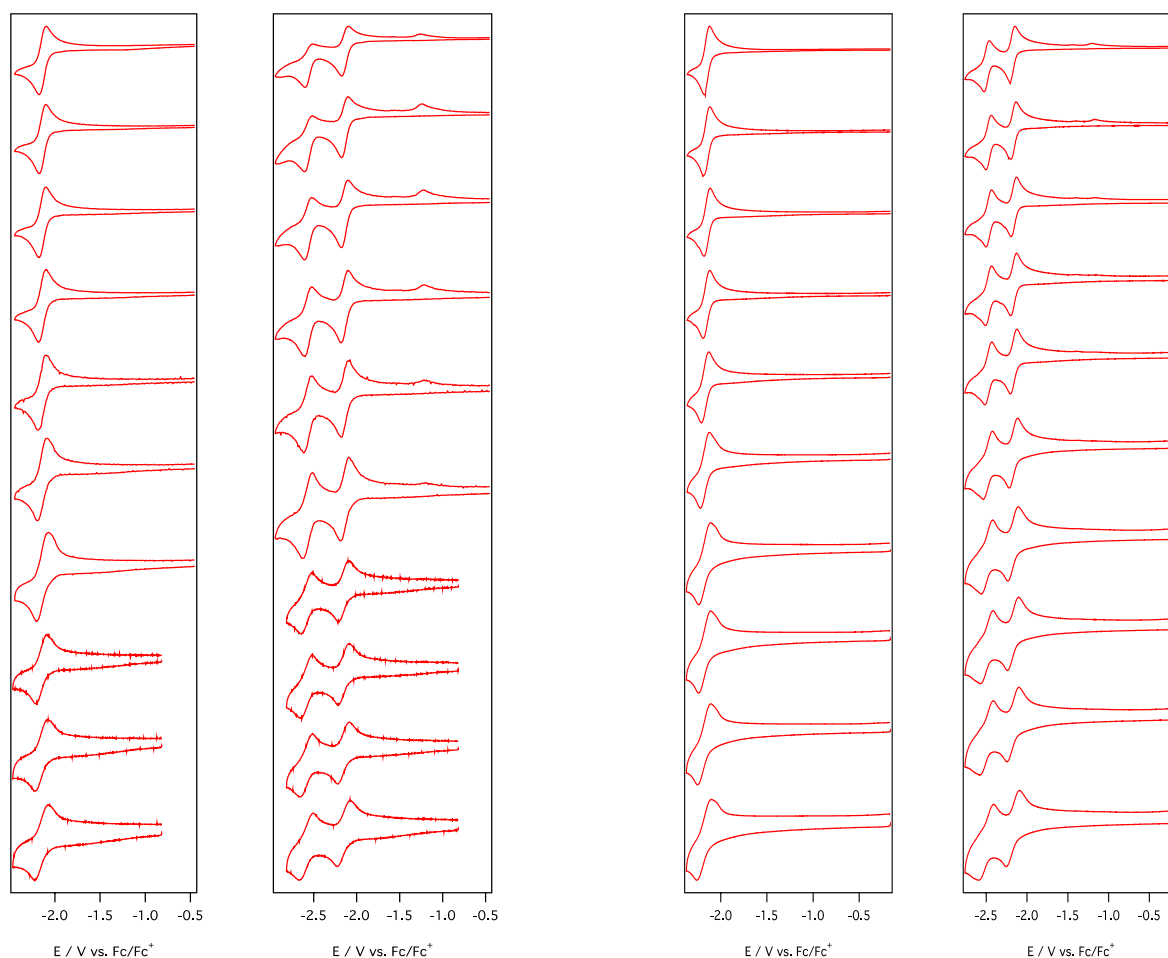


**Figure S16a:** Cyclic voltammograms of **5** at 20 °C. Scan rates ( $\nu$ ) from 0.1 V s<sup>-1</sup>, 0.2 V s<sup>-1</sup>, 0.5 V s<sup>-1</sup>, 1.0 V s<sup>-1</sup>, 2.0 V s<sup>-1</sup>, 5 V s<sup>-1</sup>, 10 V s<sup>-1</sup>, 12 V s<sup>-1</sup>, 15 V s<sup>-1</sup> and 20 V s<sup>-1</sup> (top to bottom) obtained at a glassy carbon electrode in CH<sub>3</sub>CN (0.2 M Bu<sub>4</sub>NPF<sub>6</sub>) for the 1-electron reduction (left) and 2-electron reduction (right) of *ca.* 2 mM analyte. Current data were scaled by multiplying by  $\nu^{-0.5}$ .

**Figure S16b:** Cyclic voltammograms of **5** at -30 °C. Scan rates ( $\nu$ ) from 0.1 V s<sup>-1</sup>, 0.2 V s<sup>-1</sup>, 0.5 V s<sup>-1</sup>, 1.0 V s<sup>-1</sup>, 2.0 V s<sup>-1</sup>, 5 V s<sup>-1</sup>, 10 V s<sup>-1</sup>, 12 V s<sup>-1</sup>, 15 V s<sup>-1</sup> and 20 V s<sup>-1</sup> (top to bottom) obtained at a glassy carbon electrode in CH<sub>3</sub>CN (0.2 M Bu<sub>4</sub>NPF<sub>6</sub>) for the 1-electron reduction (left) and 2-electron reduction (right) of *ca.* 2 mM analyte. Current data were scaled by multiplying by  $\nu^{-0.5}$ .

**Figure S17.** Cyclic voltammograms of compound **6** at 20 °C and -30 °C.

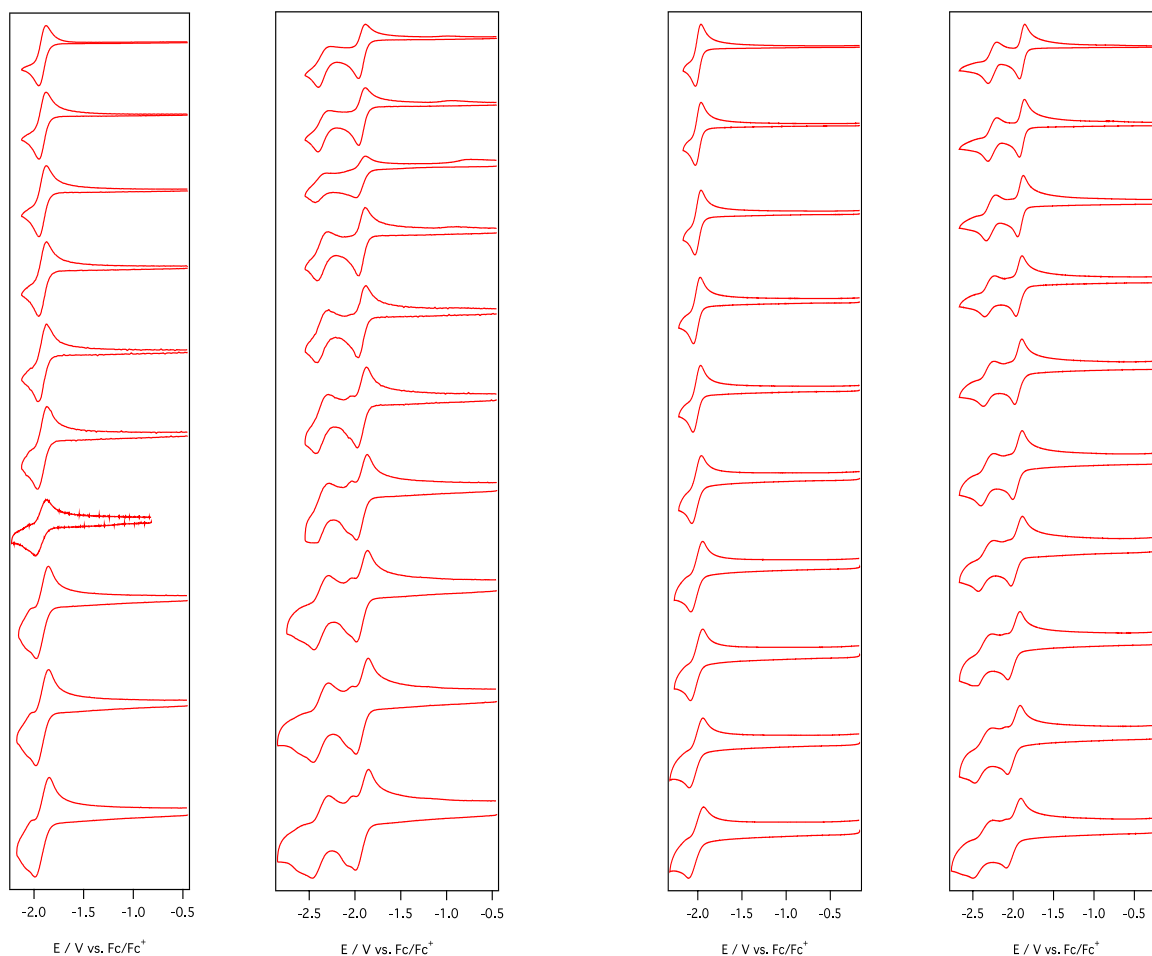


**Figure S17a:** Cyclic voltammograms of **6** at 20 °C. Scan rates ( $\nu$ ) from 0.1 V s<sup>-1</sup>, 0.2 V s<sup>-1</sup>, 0.5 V s<sup>-1</sup>, 1.0 V s<sup>-1</sup>, 2.0 V s<sup>-1</sup>, 5 V s<sup>-1</sup>, 10 V s<sup>-1</sup>, 12 V s<sup>-1</sup>, 15 V s<sup>-1</sup> and 20 V s<sup>-1</sup> (top to bottom) obtained at a glassy carbon electrode in CH<sub>3</sub>CN (0.2 M Bu<sub>4</sub>NPF<sub>6</sub>) for the 1-electron reduction (left) and 2-electron reduction (right) of *ca.* 2 mM analyte. Current data were scaled by multiplying by  $\nu^{0.5}$ .

**Figure S17b:** Cyclic voltammograms of **6** at -30 °C. Scan rates ( $\nu$ ) from 0.1 V s<sup>-1</sup>, 0.2 V s<sup>-1</sup>, 0.5 V s<sup>-1</sup>, 1.0 V s<sup>-1</sup>, 2.0 V s<sup>-1</sup>, 5 V s<sup>-1</sup>, 10 V s<sup>-1</sup>, 12 V s<sup>-1</sup>, 15 V s<sup>-1</sup> and 20 V s<sup>-1</sup> (top to bottom) obtained at a glassy carbon electrode in CH<sub>3</sub>CN (0.2 M Bu<sub>4</sub>NPF<sub>6</sub>) for the 1-electron reduction (left) and 2-electron reduction (right) of *ca.* 2 mM analyte. Current data were scaled by multiplying by  $\nu^{0.5}$ .

**Figure S18.** Cyclic voltammograms of compound **7** at 20 °C and -30 °C.

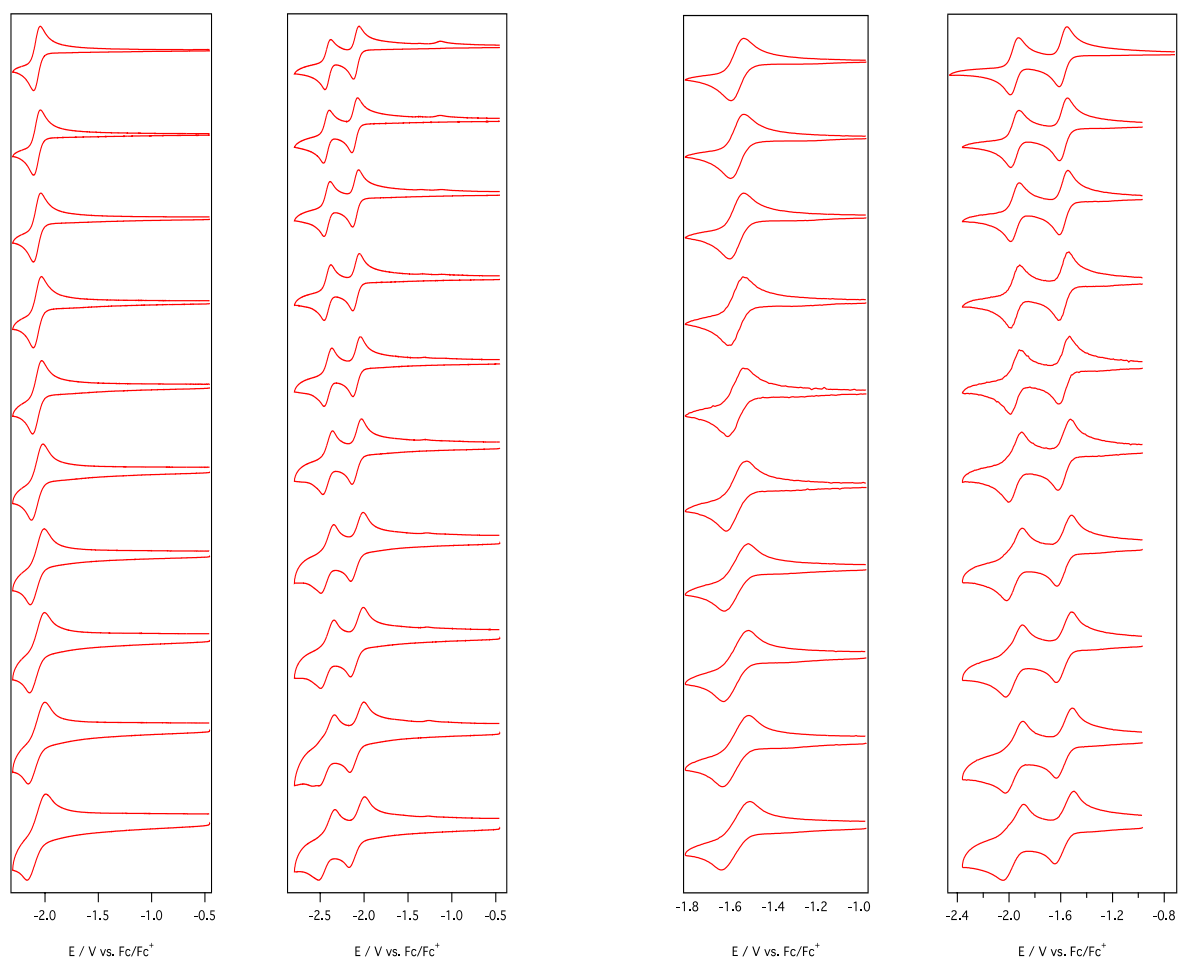


**Figure S18a:** Cyclic voltammograms of **7** at 20 °C. Scan rates ( $\nu$ ) from 0.1 V s<sup>-1</sup>, 0.2 V s<sup>-1</sup>, 0.5 V s<sup>-1</sup>, 1.0 V s<sup>-1</sup>, 2.0 V s<sup>-1</sup>, 5 V s<sup>-1</sup>, 10 V s<sup>-1</sup>, 12 V s<sup>-1</sup>, 15 V s<sup>-1</sup> and 20 V s<sup>-1</sup> (top to bottom) obtained at a glassy carbon electrode in CH<sub>3</sub>CN (0.2 M Bu<sub>4</sub>NPF<sub>6</sub>) for the 1-electron reduction (left) and 2-electron reduction (right) of *ca.* 2 mM analyte. Current data were scaled by multiplying by  $\nu^{0.5}$ .

**Figure S18b:** Cyclic voltammograms of **7** at -30 °C. Scan rates ( $\nu$ ) from 0.1 V s<sup>-1</sup>, 0.2 V s<sup>-1</sup>, 0.5 V s<sup>-1</sup>, 1.0 V s<sup>-1</sup>, 2.0 V s<sup>-1</sup>, 5 V s<sup>-1</sup>, 10 V s<sup>-1</sup>, 12 V s<sup>-1</sup>, 15 V s<sup>-1</sup> and 20 V s<sup>-1</sup> (top to bottom) obtained at a glassy carbon electrode in CH<sub>3</sub>CN (0.2 M Bu<sub>4</sub>NPF<sub>6</sub>) for the 1-electron reduction (left) and 2-electron reduction (right) of *ca.* 2 mM analyte. Current data were scaled by multiplying by  $\nu^{0.5}$ .

**Figure S19.** Cyclic voltammograms of compound **8** at 20 °C and -30 °C.

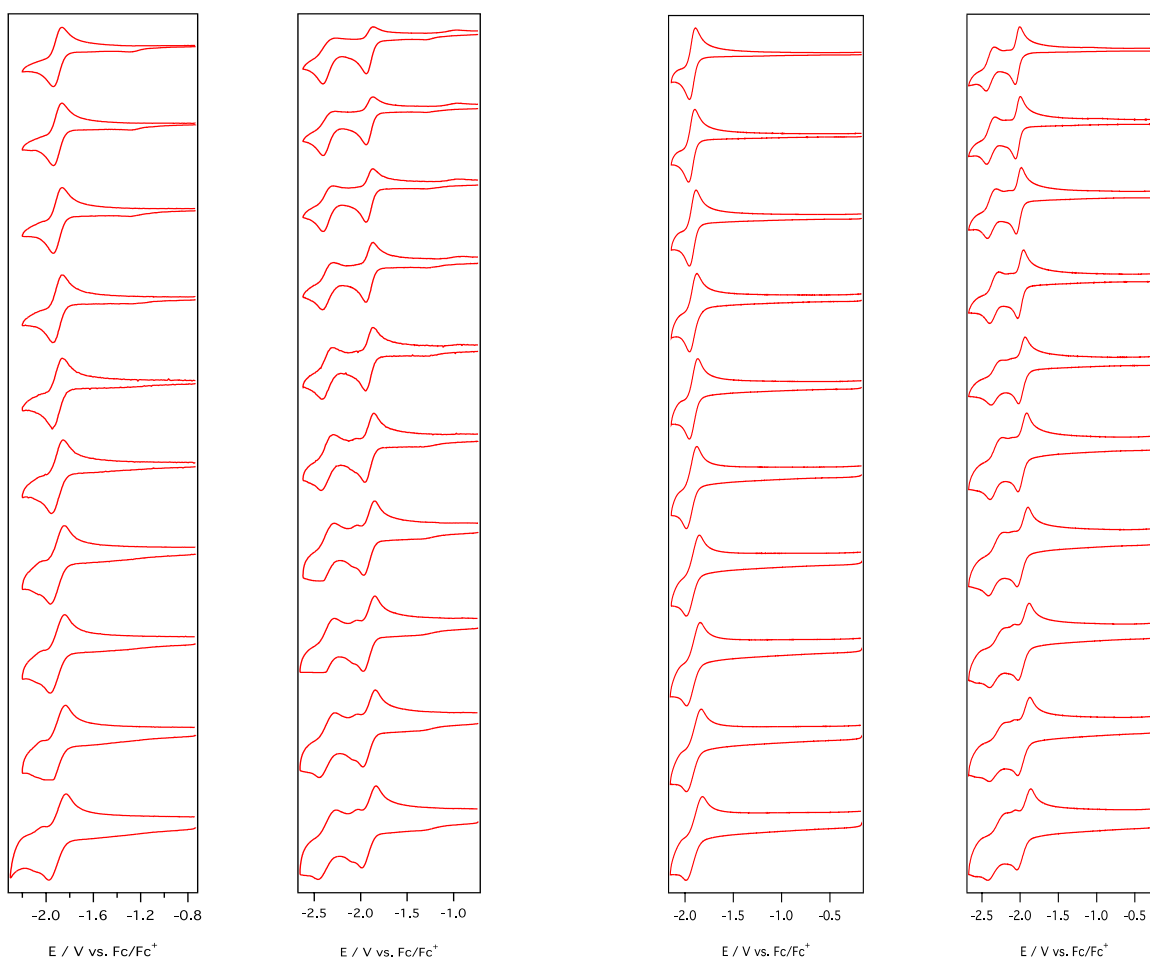


**Figure S19a:** Cyclic voltammograms of **8** at 20 °C. Scan rates ( $\nu$ ) from 0.1 V s<sup>-1</sup>, 0.2 V s<sup>-1</sup>, 0.5 V s<sup>-1</sup>, 1.0 V s<sup>-1</sup>, 2.0 V s<sup>-1</sup>, 5 V s<sup>-1</sup>, 10 V s<sup>-1</sup>, 12 V s<sup>-1</sup>, 15 V s<sup>-1</sup> and 20 V s<sup>-1</sup> (top to bottom) obtained at a glassy carbon electrode in CH<sub>3</sub>CN (0.2 M Bu<sub>4</sub>NPF<sub>6</sub>) for the 1-electron reduction (left) and 2-electron reduction (right) of *ca.* 2 mM analyte. Current data were scaled by multiplying by  $\nu^{0.5}$ .

**Figure S19b:** Cyclic voltammograms of **8** at -30 °C. Scan rates ( $\nu$ ) from 0.1 V s<sup>-1</sup>, 0.2 V s<sup>-1</sup>, 0.5 V s<sup>-1</sup>, 1.0 V s<sup>-1</sup>, 2.0 V s<sup>-1</sup>, 5 V s<sup>-1</sup>, 10 V s<sup>-1</sup>, 12 V s<sup>-1</sup>, 15 V s<sup>-1</sup> and 20 V s<sup>-1</sup> (top to bottom) obtained at a glassy carbon electrode in CH<sub>3</sub>CN (0.2 M Bu<sub>4</sub>NPF<sub>6</sub>) for the 1-electron reduction (left) and 2-electron reduction (right) of *ca.* 2 mM analyte. Current data were scaled by multiplying by  $\nu^{0.5}$ .

**Figure S20.** Cyclic voltammograms of compound **9** at 20 °C and -30 °C.

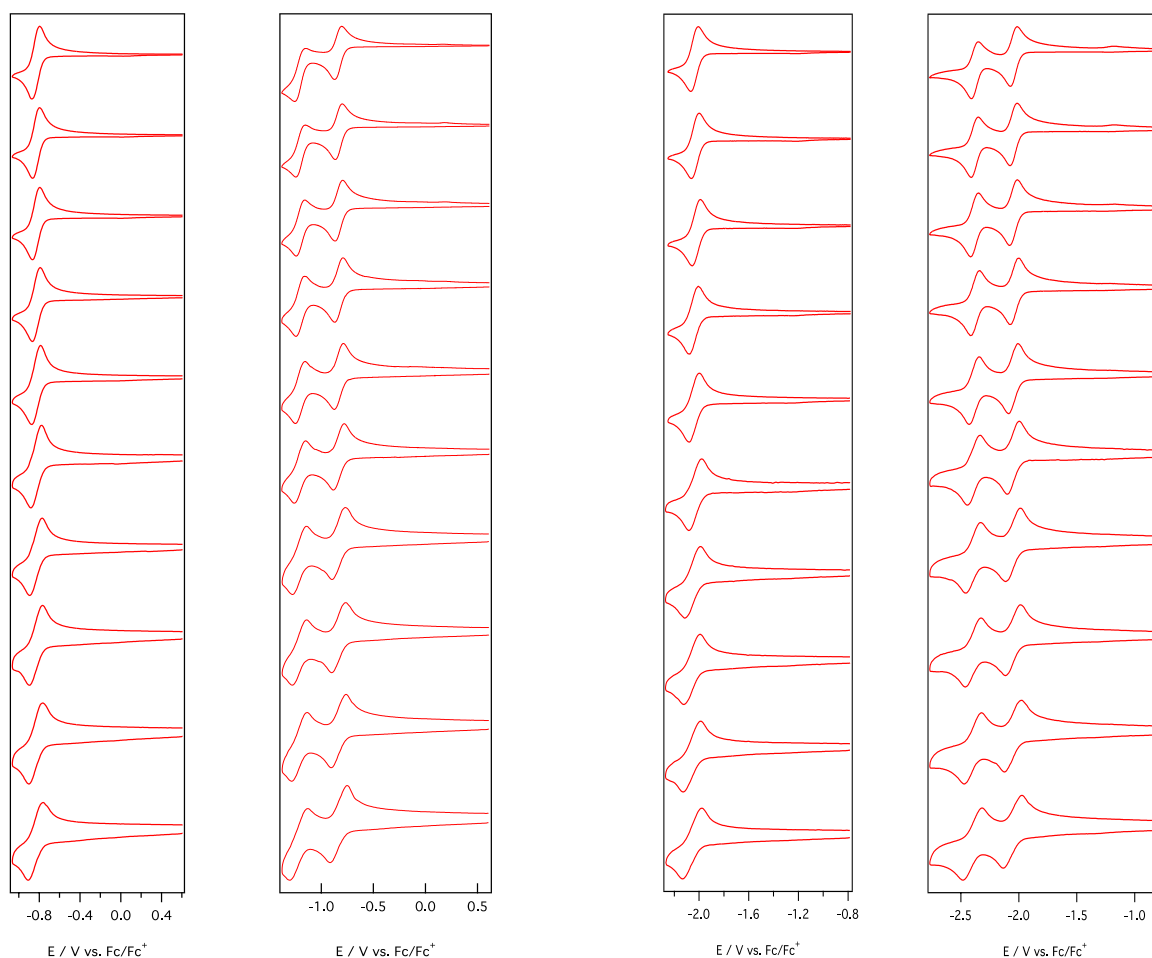


**Figure S20a:** Cyclic voltammograms of **9** at 20 °C. Scan rates ( $\nu$ ) from 0.1 V s<sup>-1</sup>, 0.2 V s<sup>-1</sup>, 0.5 V s<sup>-1</sup>, 1.0 V s<sup>-1</sup>, 2.0 V s<sup>-1</sup>, 5 V s<sup>-1</sup>, 10 V s<sup>-1</sup>, 12 V s<sup>-1</sup>, 15 V s<sup>-1</sup> and 20 V s<sup>-1</sup> (top to bottom) obtained at a glassy carbon electrode in CH<sub>3</sub>CN (0.2 M Bu<sub>4</sub>NPF<sub>6</sub>) for the 1-electron reduction (left) and 2-electron reduction (right) of *ca.* 2 mM analyte. Current data were scaled by multiplying by  $\nu^{0.5}$ .

**Figure S20b:** Cyclic voltammograms of **9** at -30 °C. Scan rates ( $\nu$ ) from 0.1 V s<sup>-1</sup>, 0.2 V s<sup>-1</sup>, 0.5 V s<sup>-1</sup>, 1.0 V s<sup>-1</sup>, 2.0 V s<sup>-1</sup>, 5 V s<sup>-1</sup>, 10 V s<sup>-1</sup>, 12 V s<sup>-1</sup>, 15 V s<sup>-1</sup> and 20 V s<sup>-1</sup> (top to bottom) obtained at a glassy carbon electrode in CH<sub>3</sub>CN (0.2 M Bu<sub>4</sub>NPF<sub>6</sub>) for the 1-electron reduction (left) and 2-electron reduction (right) of *ca.* 2 mM analyte. Current data were scaled by multiplying by  $\nu^{0.5}$ .

**Figure S21.** Cyclic voltammograms of compound **10** at 20 °C.

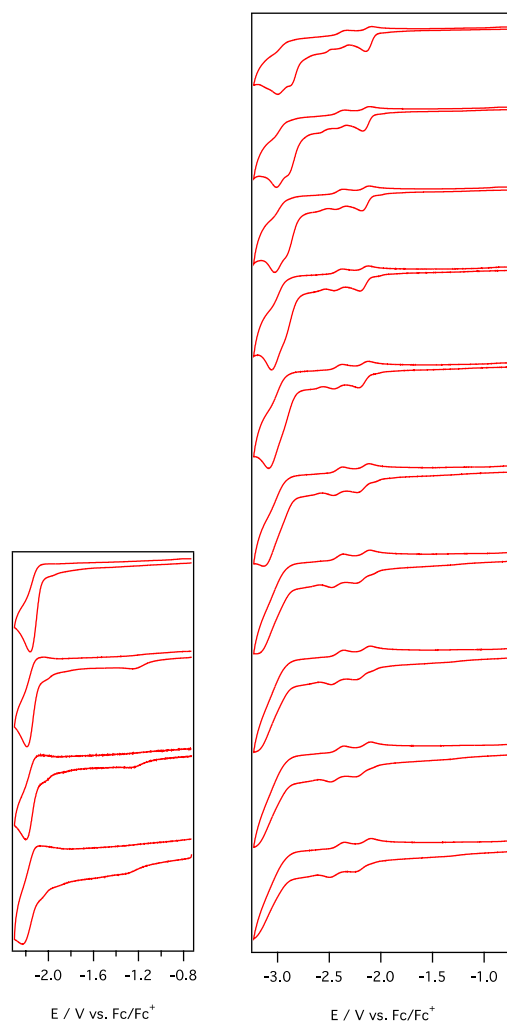


**Figure S21:** Cyclic voltammograms of **10** at 20 °C. Scan rates ( $\nu$ ) from 0.1 V s<sup>-1</sup>, 0.2 V s<sup>-1</sup>, 0.5 V s<sup>-1</sup>, 1.0 V s<sup>-1</sup>, 2.0 V s<sup>-1</sup>, 5 V s<sup>-1</sup>, 10 V s<sup>-1</sup>, 12 V s<sup>-1</sup>, 15 V s<sup>-1</sup> and 20 V s<sup>-1</sup> (top to bottom) obtained at a glassy carbon electrode in DMF (0.2 M Bu<sub>4</sub>NPF<sub>6</sub>) for the 1-electron reduction (left) and 2-electron reduction (right) of *ca.* 2 mM analyte. Current data were scaled by multiplying by  $\nu^{0.5}$ .

**Figure S22.** Cyclic voltammograms of compound **11** at 20 °C.

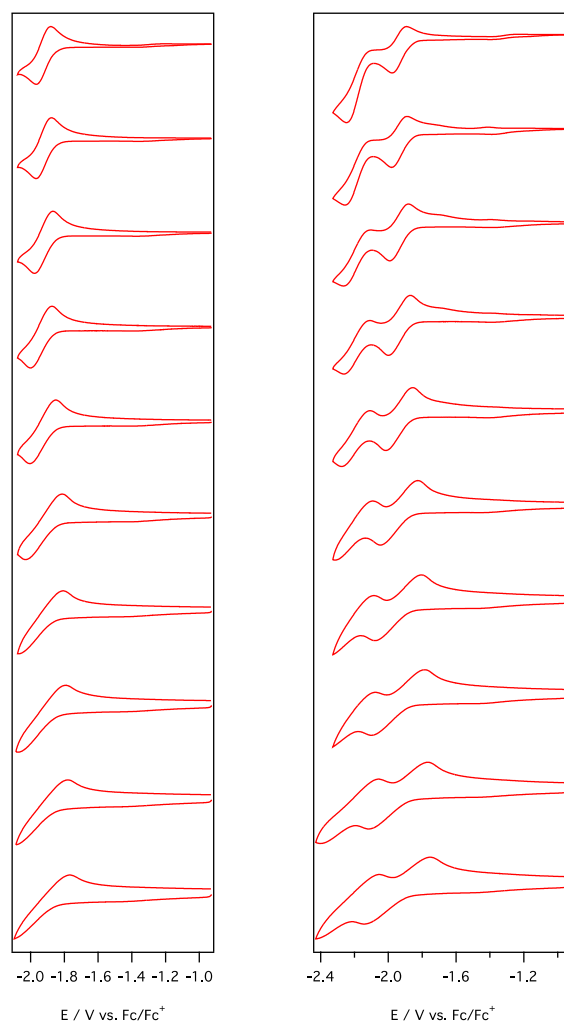


**Figure S22:** Cyclic voltammograms of **11** at 20 °C. Scan rates ( $\nu$ ) from 0.1 V s<sup>-1</sup>, 0.2 V s<sup>-1</sup>, 0.5 V s<sup>-1</sup>, 1.0 V s<sup>-1</sup>, 2.0 V s<sup>-1</sup>, 5 V s<sup>-1</sup>, 10 V s<sup>-1</sup>, 12 V s<sup>-1</sup>, 15 V s<sup>-1</sup> and 20 V s<sup>-1</sup> (top to bottom) obtained at a glassy carbon electrode in DCM (0.2 M Bu<sub>4</sub>NPF<sub>6</sub>) for the 1-electron reduction (left) and 2-electron reduction (right) of *ca.* 2 mM analyte. Current data were scaled by multiplying by  $\nu^{0.5}$ .

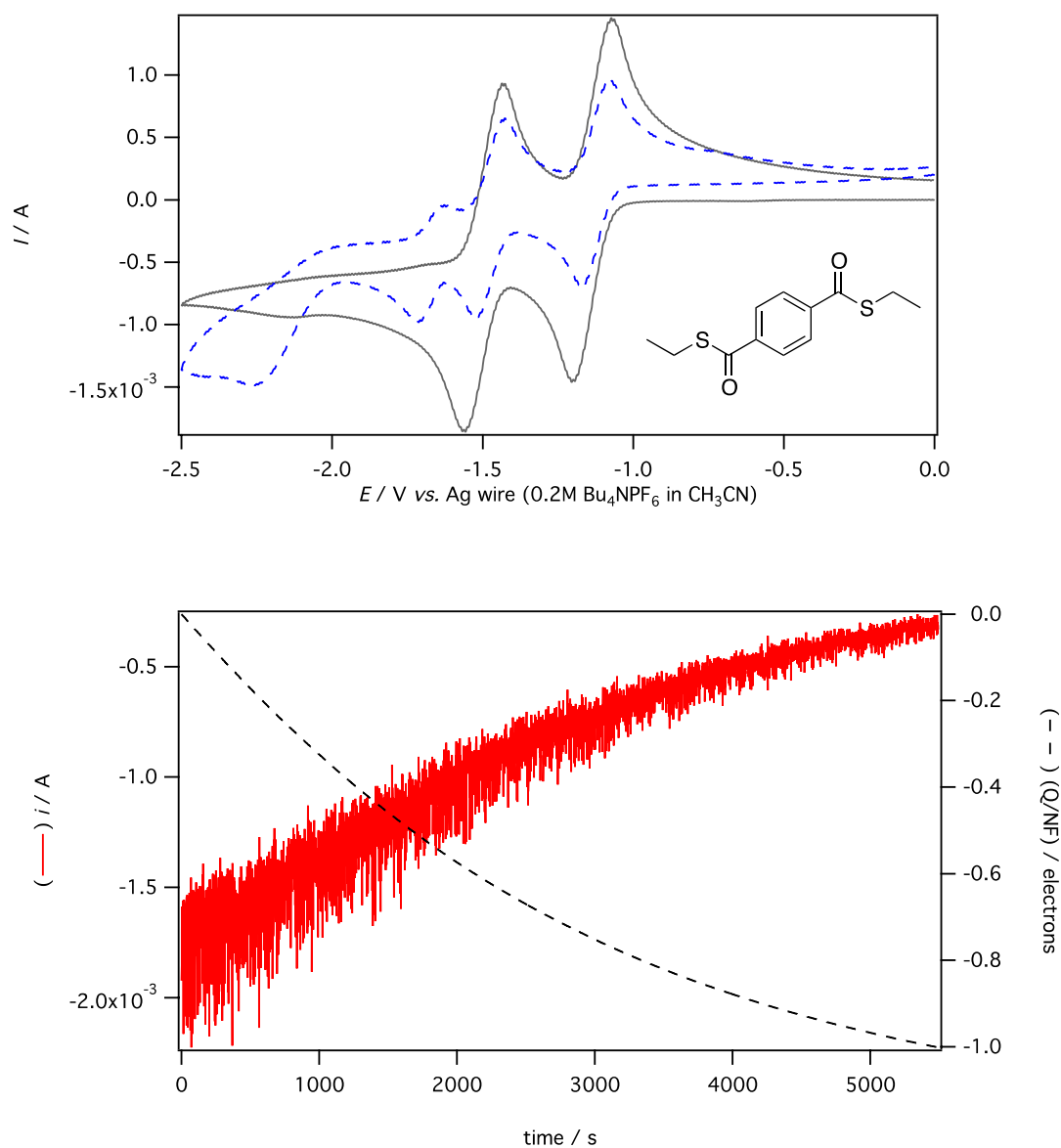


**Figure S23.** Voltammetric and coulometric data of *S,S*-diethyl benzene-1,4-bis(carbothioate) (compound **1**). (—) Before electrolysis. (---) After one-electron reduction.

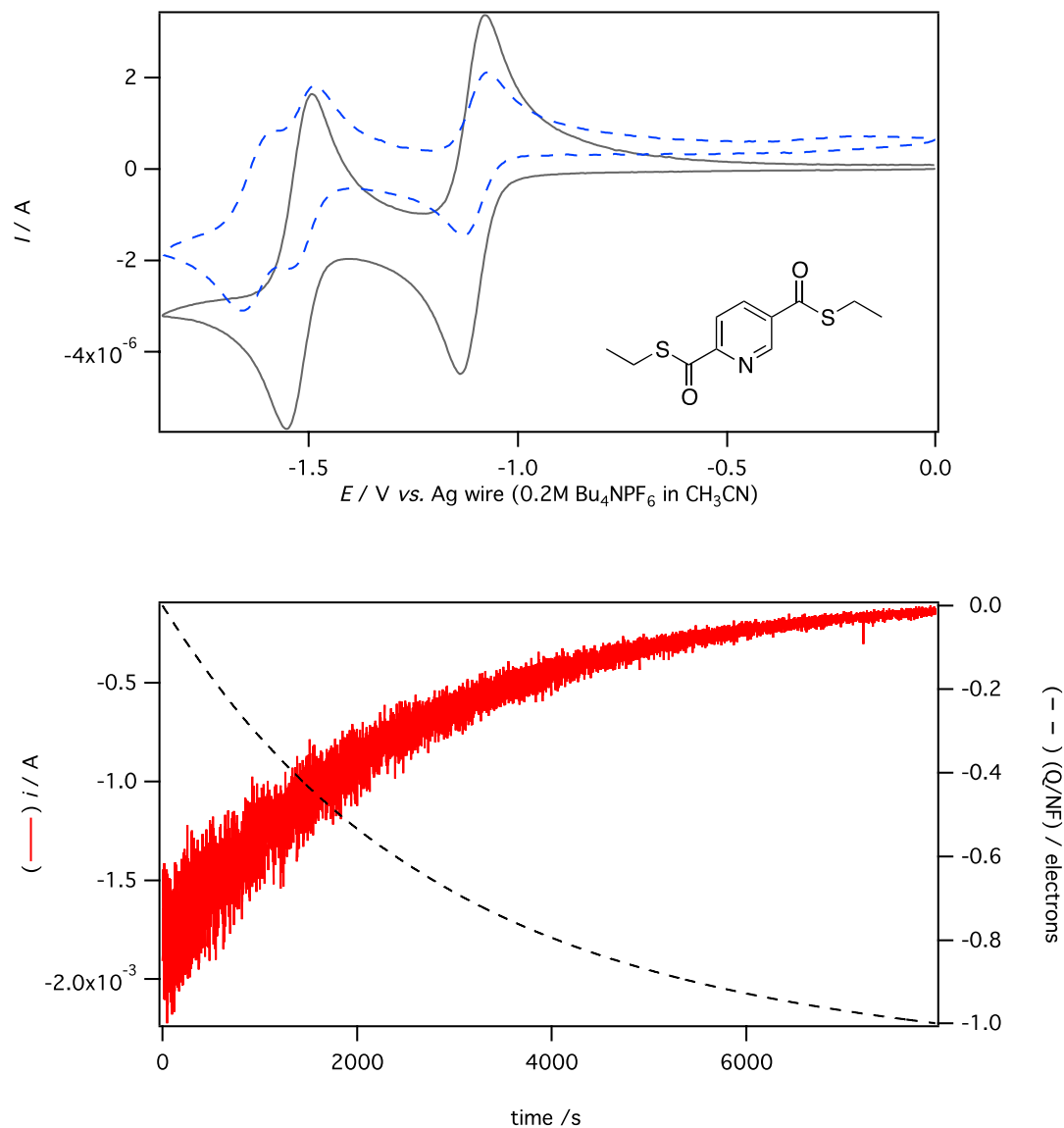


**Figure S24.** Voltammetric and coulometric data of *S,S*-diethyl pyridine-2,5-bis(carbothioate) (compound **2**). (—) Before electrolysis. (---) After one-electron reduction.

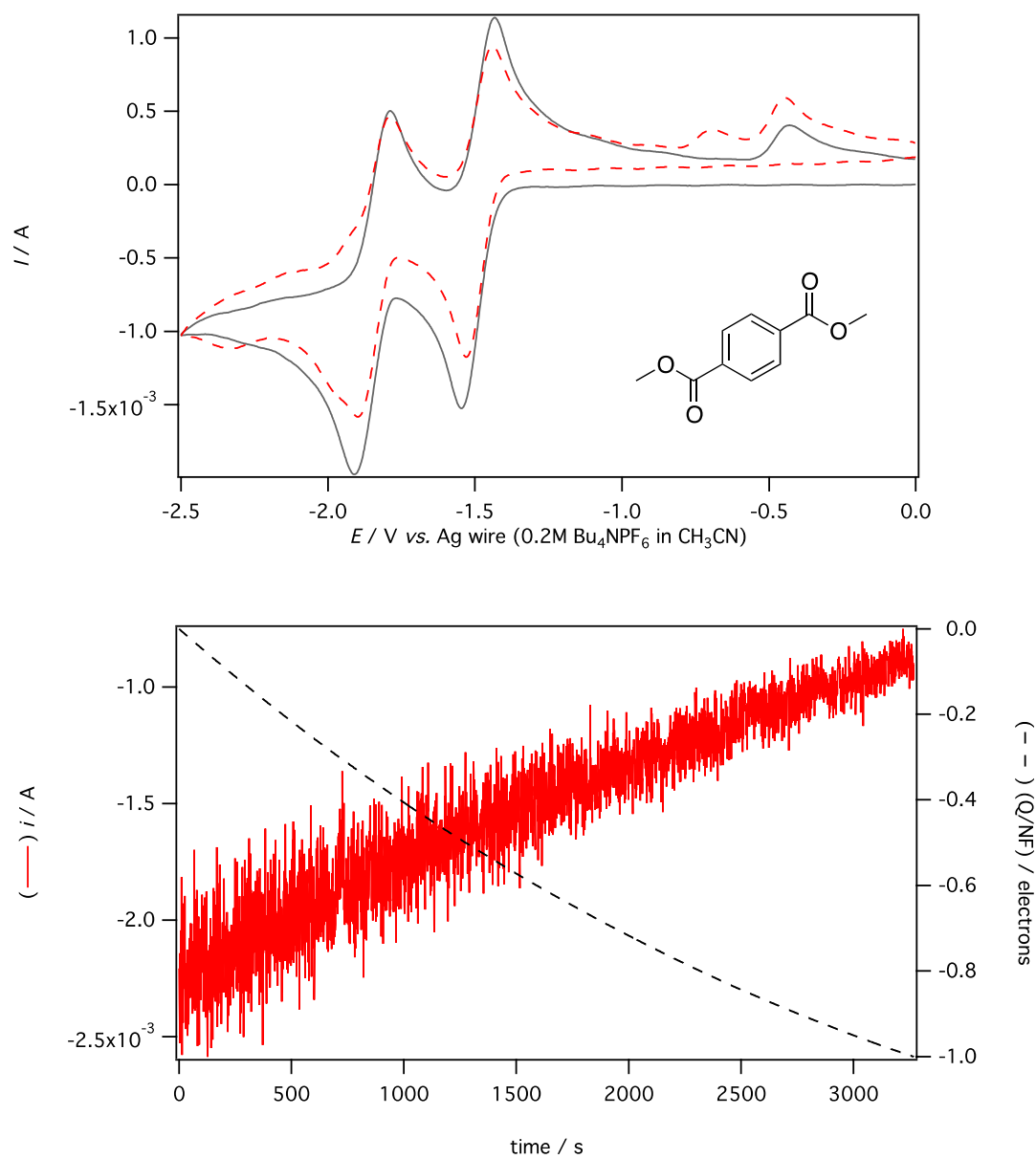


**Figure S25.** Voltammetric and coulometric data of dimethyl terephthalate (compound **3**). (—) Before electrolysis. (---) After one-electron reduction.

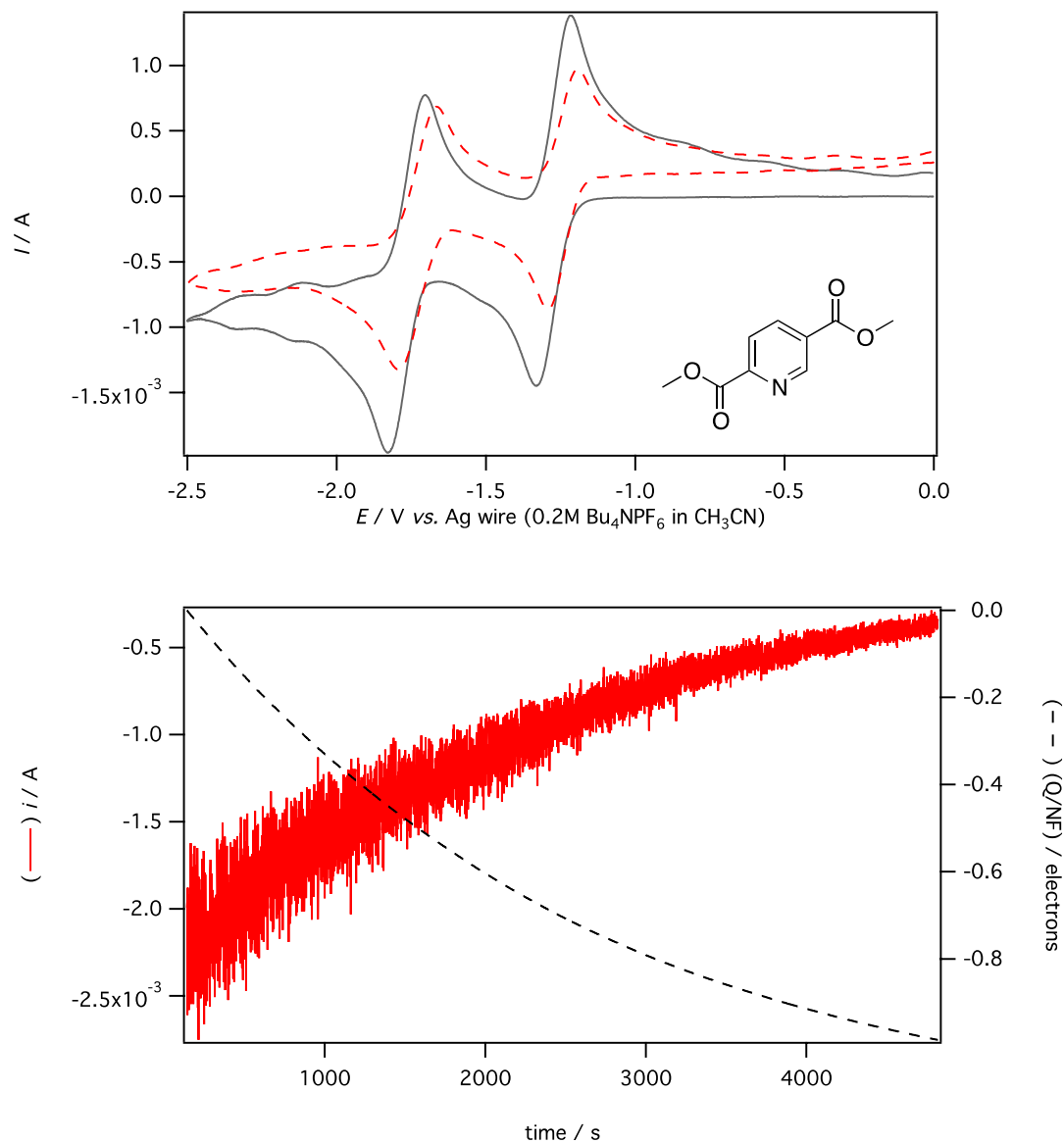


**Figure S26.** Voltammetric and coulometric data of dimethyl pyridine-2,5-dicarboxylate (compound **4**). (—) Before electrolysis. (---) After one-electron reduction.

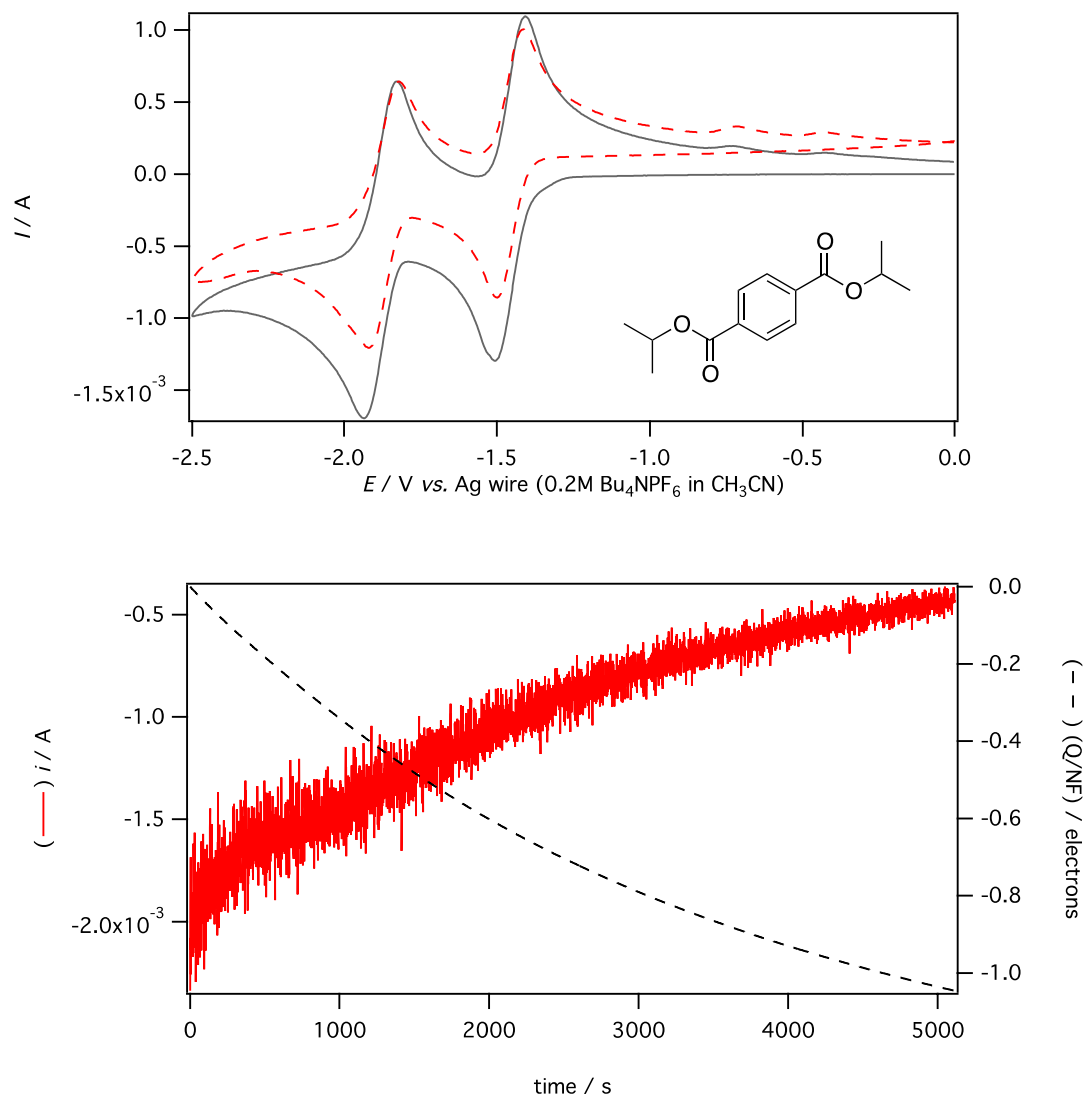


**Figure S27.** Voltammetric and coulometric data of diisopropyl terephthalate (compound **5**). (—) Before electrolysis. (---) After one-electron reduction.

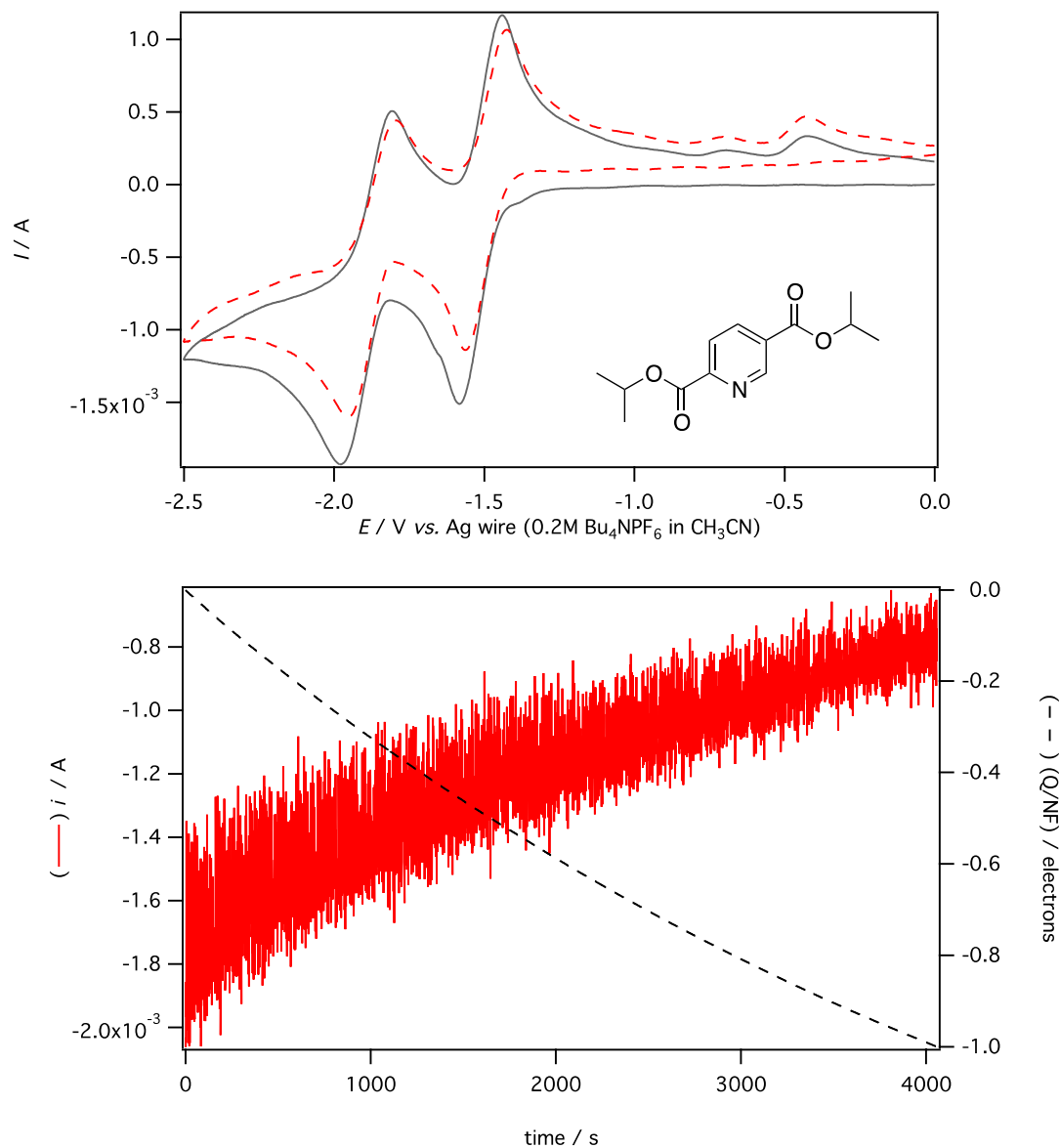


**Figure S28.** Voltammetric and coulometric data of diisopropyl pyridine-2,5-dicarboxylate (compound **6**). (—) Before electrolysis. (---) After one-electron reduction.

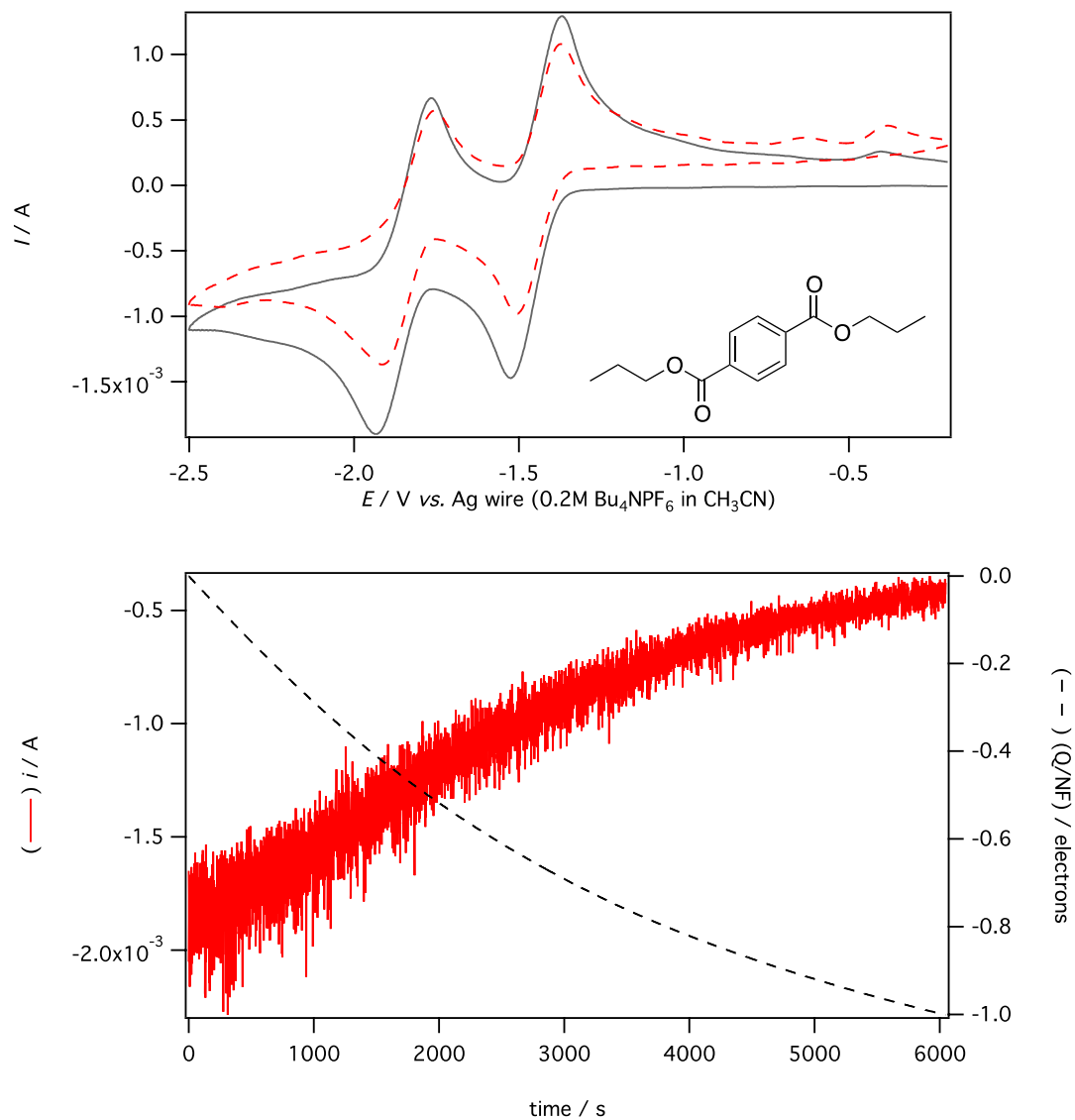


**Figure S29.** Voltammetric and coulometric data of dipropyl terephthalate (compound 7). (—) Before electrolysis. (---) After one-electron reduction.

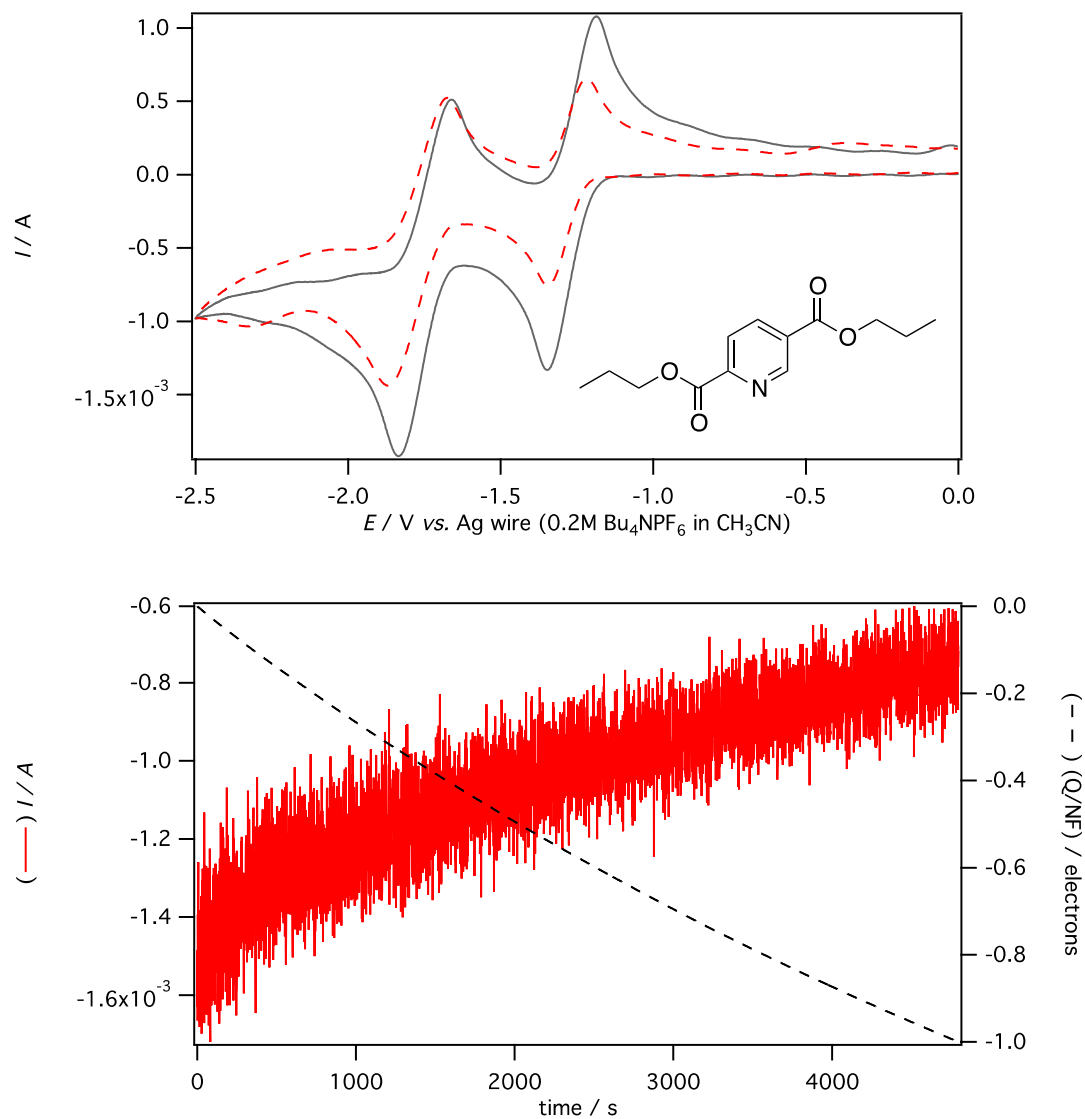


**Figure S30.** Voltammetric and coulometric data of dipropyl pyridine-2,5-dicarboxylate (compound **8**). (—) Before electrolysis. (---) After one-electron reduction.

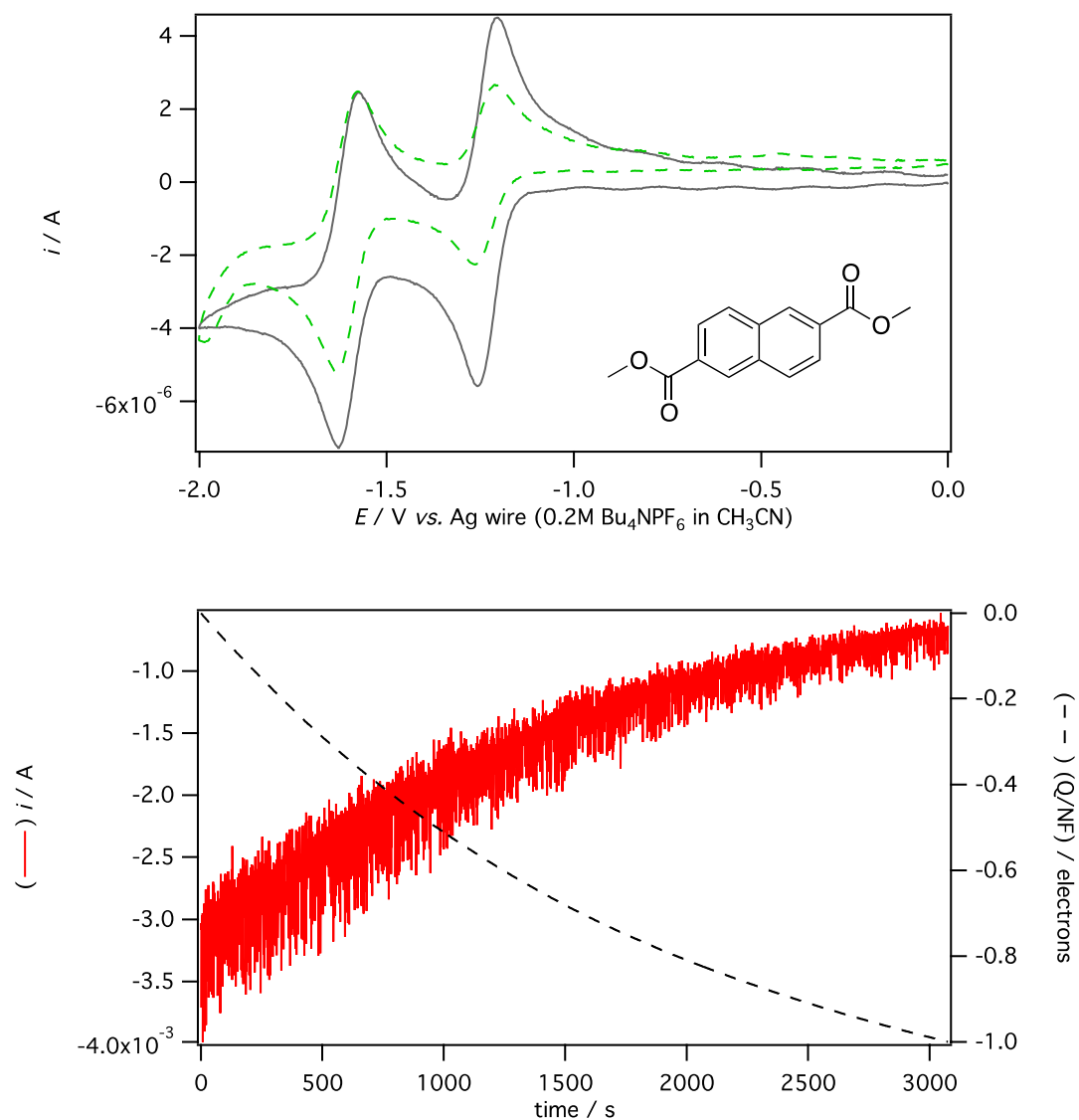


**Figure S31.** Voltammetric and coulometric data of dimethyl naphthalene-2,6-dicarboxylate (compound **9**). (—) Before electrolysis. (---) After one-electron reduction.

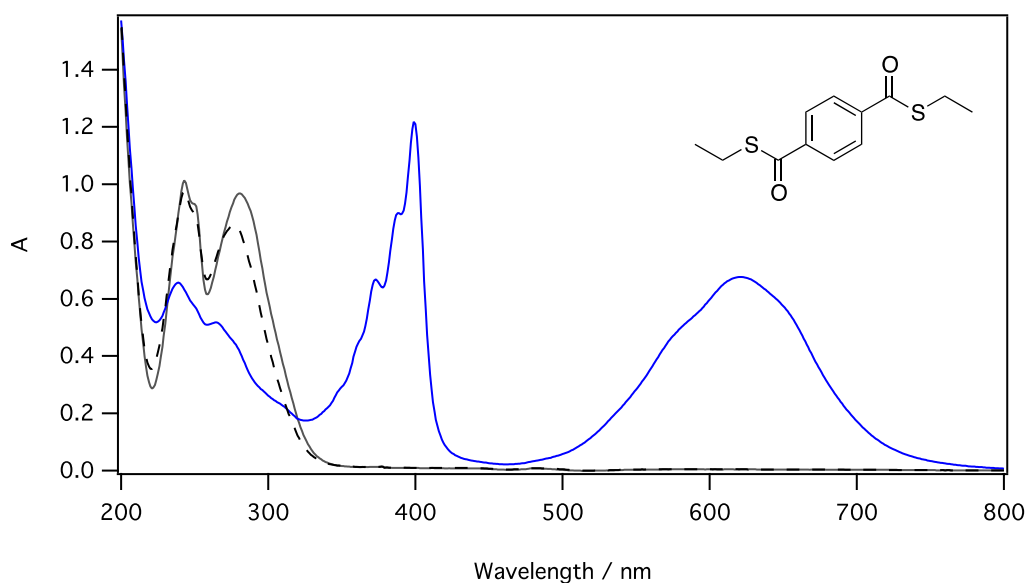


**Figure S32.** *In situ* electrochemical UV-vis spectra obtained at a Pt mesh electrode of *S,S*-diethyl benzene-1,4-bis(carbothioate) (compound **1**). (—) Before electrolysis. (—) After one-electron reduction. (---) After re-oxidation back to starting material.

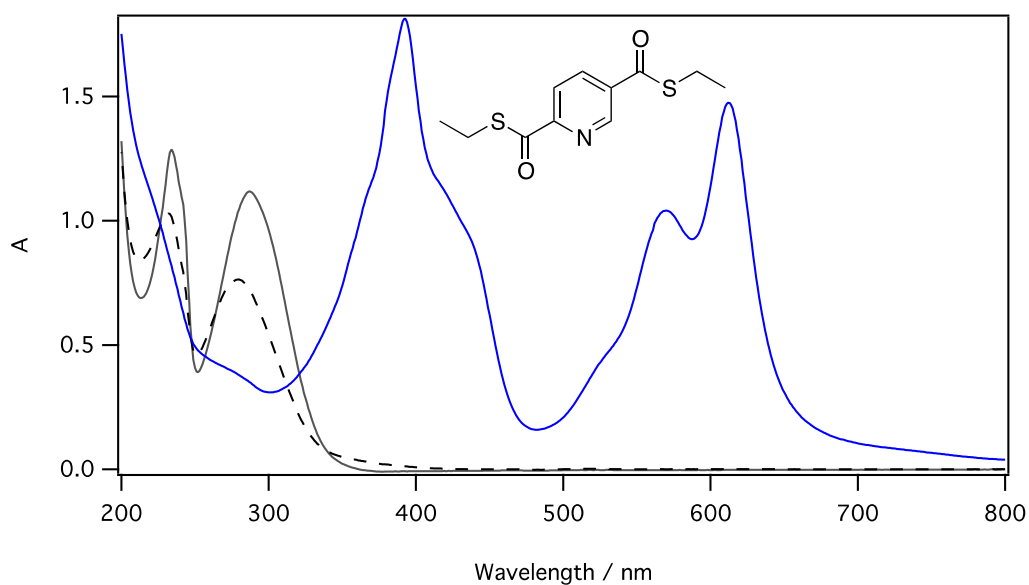


**Figure S33.** *In situ* electrochemical UV-vis spectra obtained at a Pt mesh electrode of *S,S*-diethyl pyridine-2,5-bis(carbothioate) (compound **2**). (—) Before electrolysis. (—) After one-electron reduction. (---) After re-oxidation back to starting material.

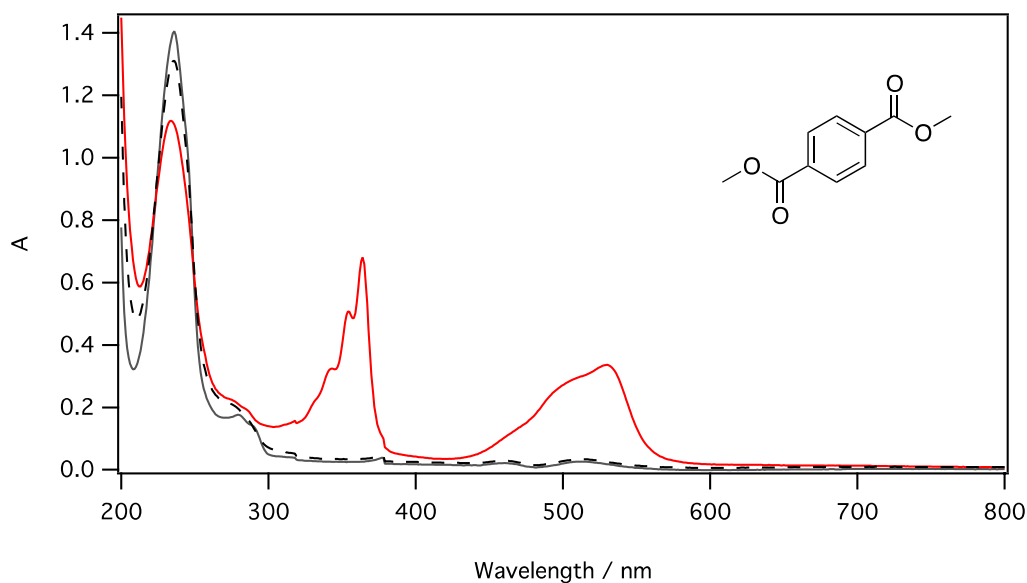


**Figure S34.** *In situ* electrochemical UV-vis spectra obtained at a Pt mesh electrode of dimethyl terephthalate (compound **3**). (—) Before electrolysis. (—) After one-electron reduction. (---) After re-oxidation back to starting material.

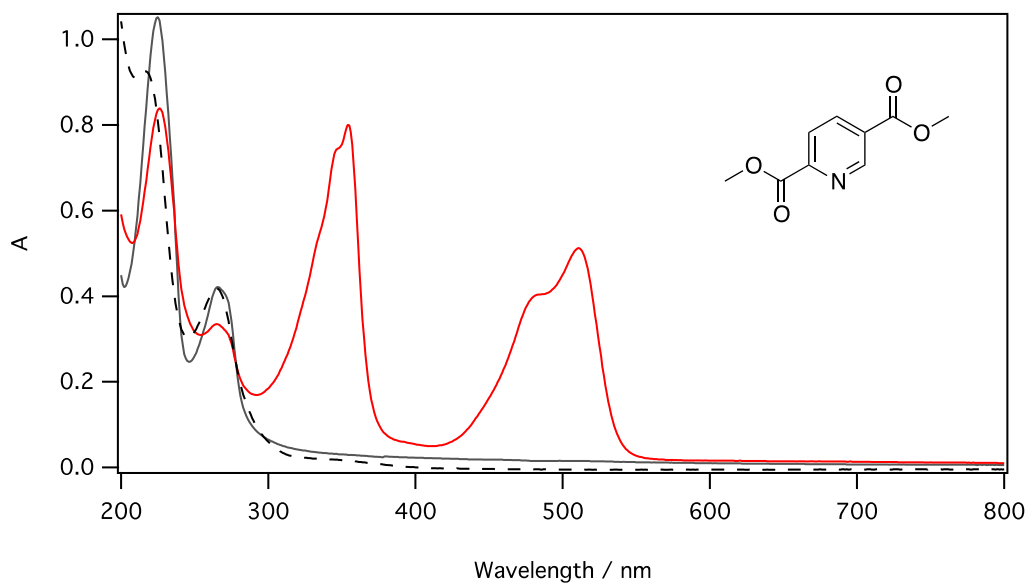


**Figure S35.** *In situ* electrochemical UV-vis spectra obtained at a Pt mesh electrode of dimethyl pyridine-2,5-dicarboxylate (compound **4**). (—) Before electrolysis. (—) After one-electron reduction. (---) After re-oxidation back to starting material.

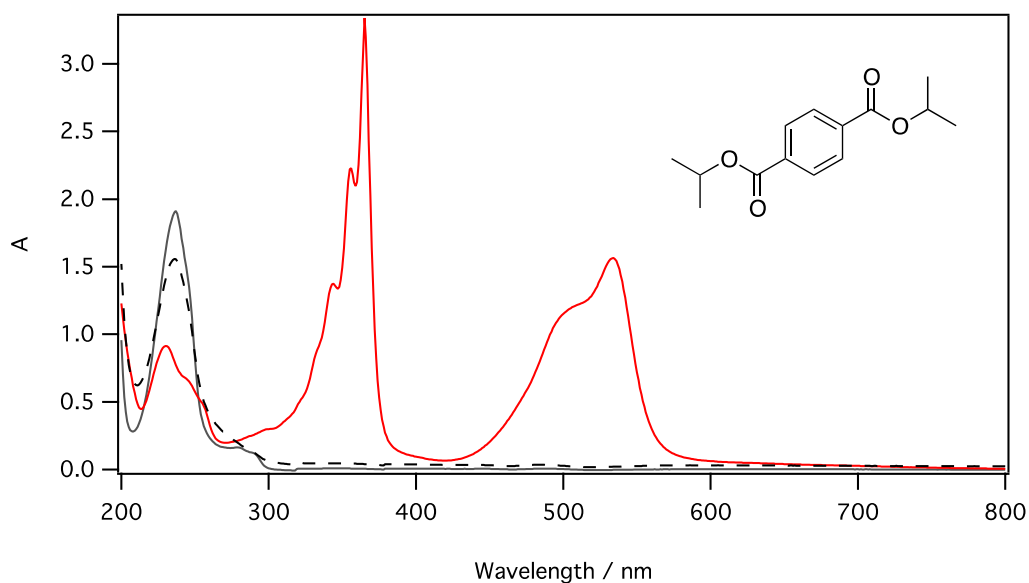


**Figure S36.** *In situ* electrochemical UV-vis spectra obtained at a Pt mesh electrode of diisopropyl terephthalate (compound **5**). (—) Before electrolysis. (—) After one-electron reduction. (---) After re-oxidation back to starting material.

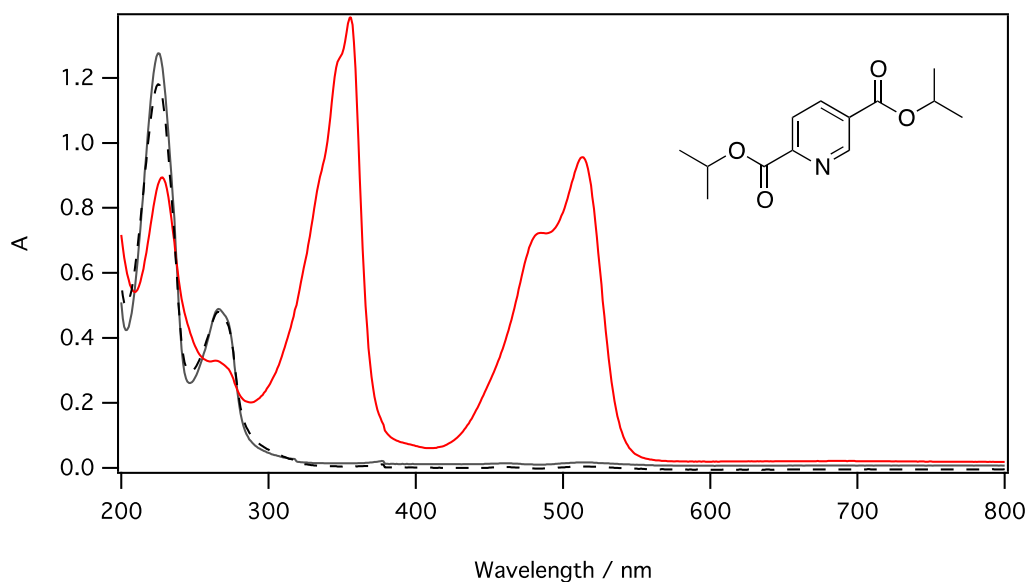


**Figure S37.** *In situ* electrochemical UV-vis spectra obtained at a Pt mesh electrode of diisopropyl pyridine-2,5-dicarboxylate (compound **6**). (—) Before electrolysis. (—) After one-electron reduction. (---) After re-oxidation back to starting material.

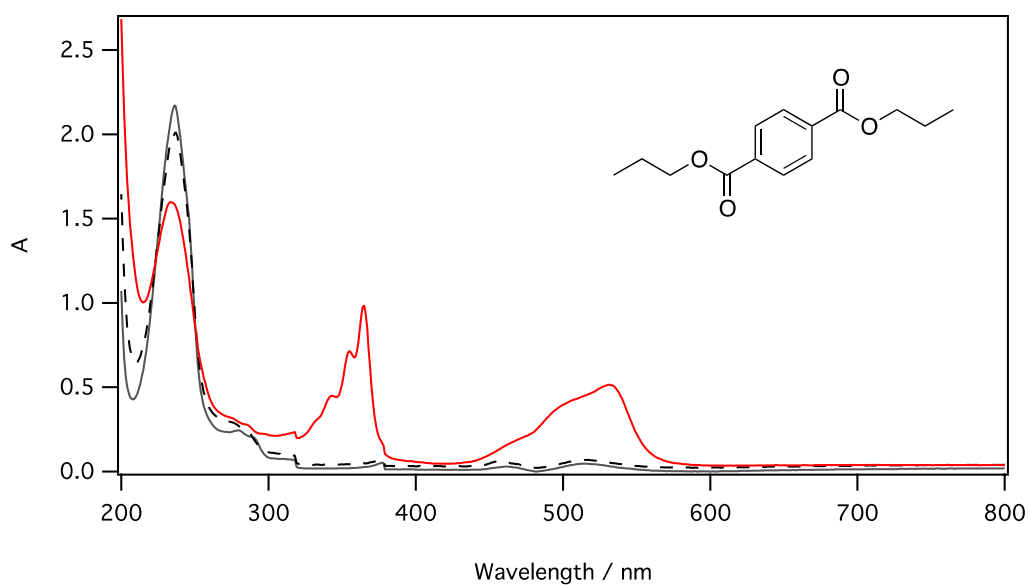


**Figure S38.** *In situ* electrochemical UV-vis spectra obtained at a Pt mesh electrode of dipropyl terephthalate (compound **7**). (—) Before electrolysis. (—) After one-electron reduction. (---) After re-oxidation back to starting material.

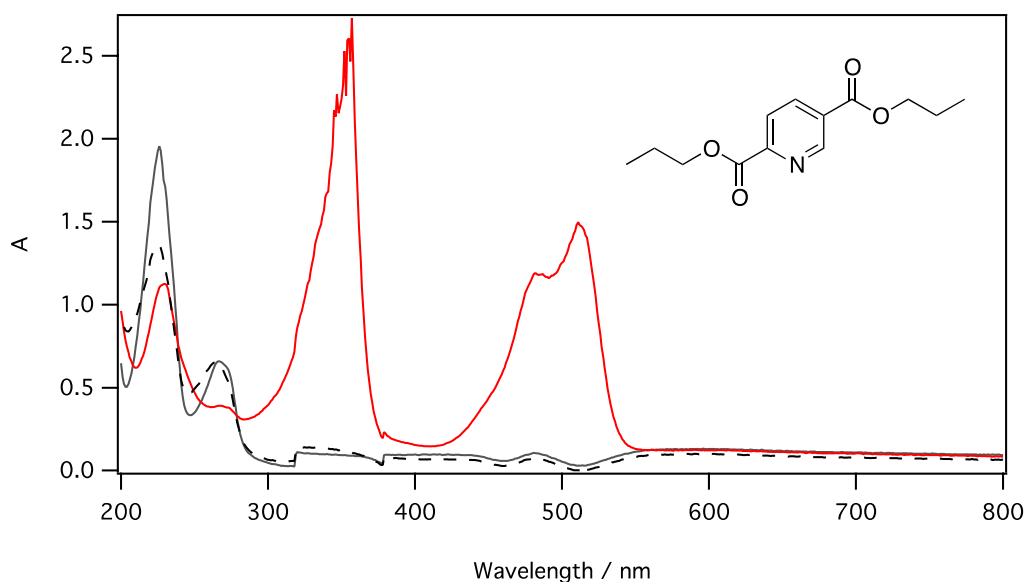


**Figure S39.** *In situ* electrochemical UV-vis spectra obtained at a Pt mesh electrode of dipropyl pyridine-2,5-dicarboxylate (compound **8**). (—) Before electrolysis. (—) After one-electron reduction. (---) After re-oxidation back to starting material.

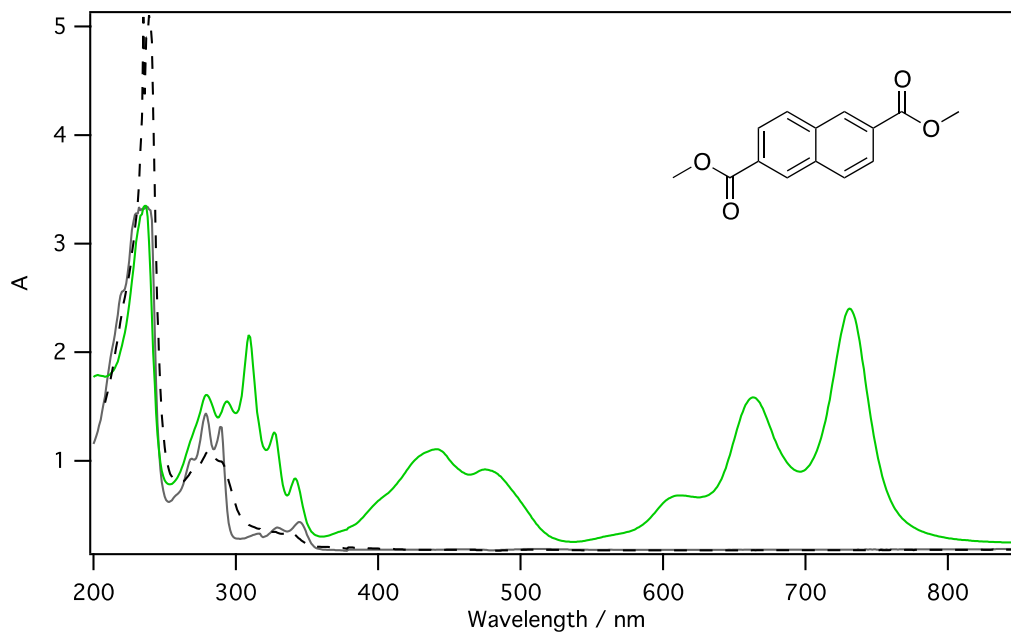


**Figure S40.** *In situ* electrochemical UV-vis spectra obtained at a Pt mesh electrode of dimethyl naphthalene-2,6-dicarboxylate (compound **9**). (—) Before electrolysis. (—) After one-electron reduction. (---) After re-oxidation back to starting material.

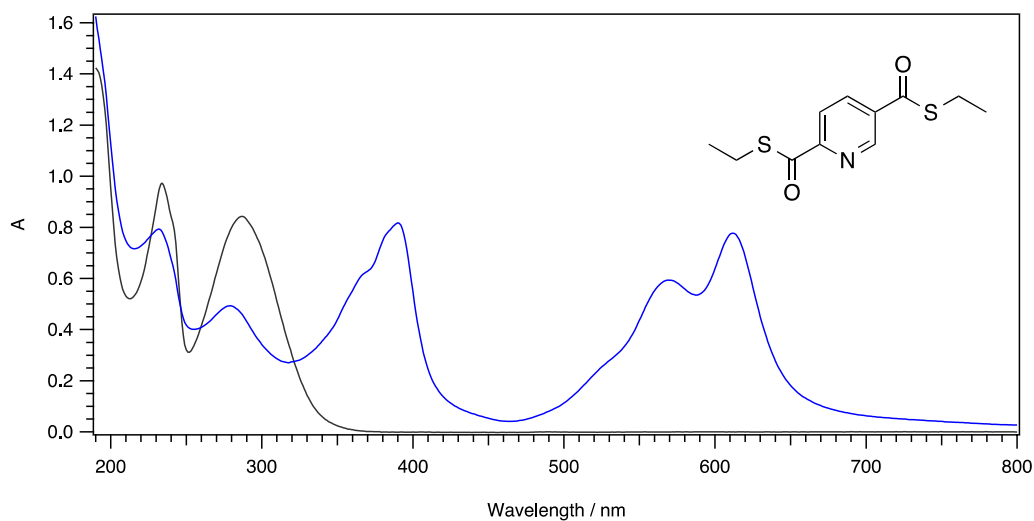


**Figure S41a.** Background subtracted *in situ* electrochemical UV-vis spectra obtained at a gold micro-mesh electrode of 1 mM *S,S*-diethyl pyridine-2,5-bis(carbothioate) (compound **2**). (—) Before electrolysis. (—) After one-electron reduction.

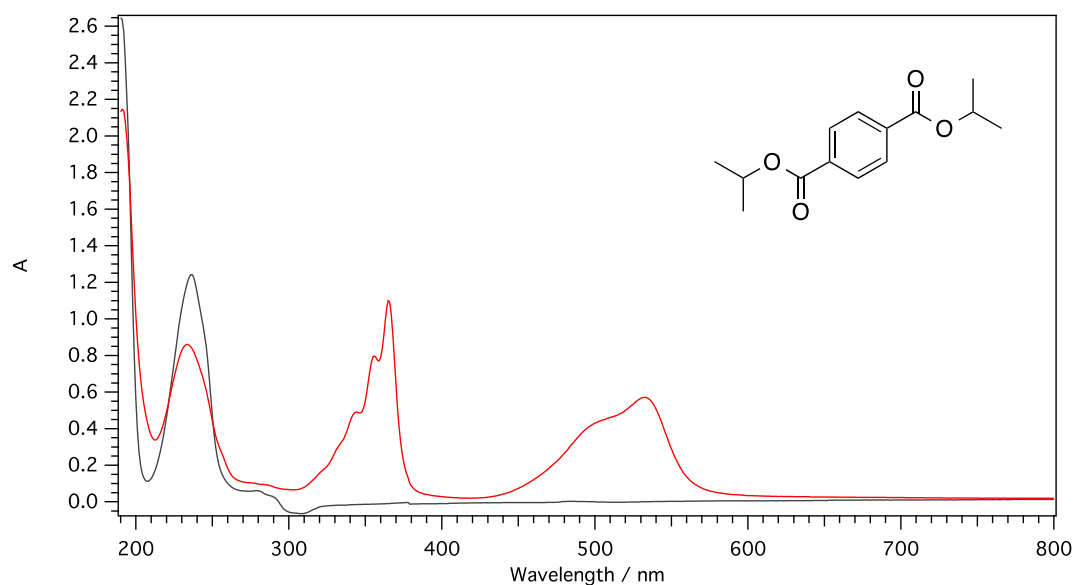


**Figure S41b.** Background subtracted *in situ* electrochemical UV-vis spectra obtained at a gold micro-mesh electrode of 1 mM diisopropyl terephthalate (compound **5**). (—) Before electrolysis. (—) After one-electron reduction.

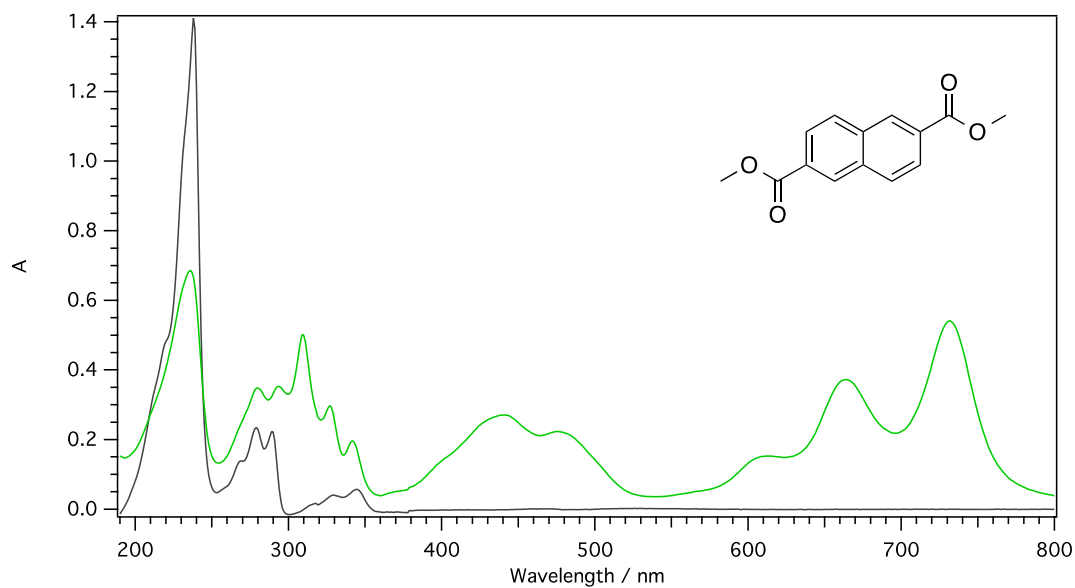


**Figure S41c.** Background subtracted *in situ* electrochemical UV-vis spectra obtained at a gold micro-mesh electrode of 1 mM dimethyl naphthalene-2,6-dicarboxylate (compound **9**). (—) Before electrolysis. (—) After one-electron reduction.

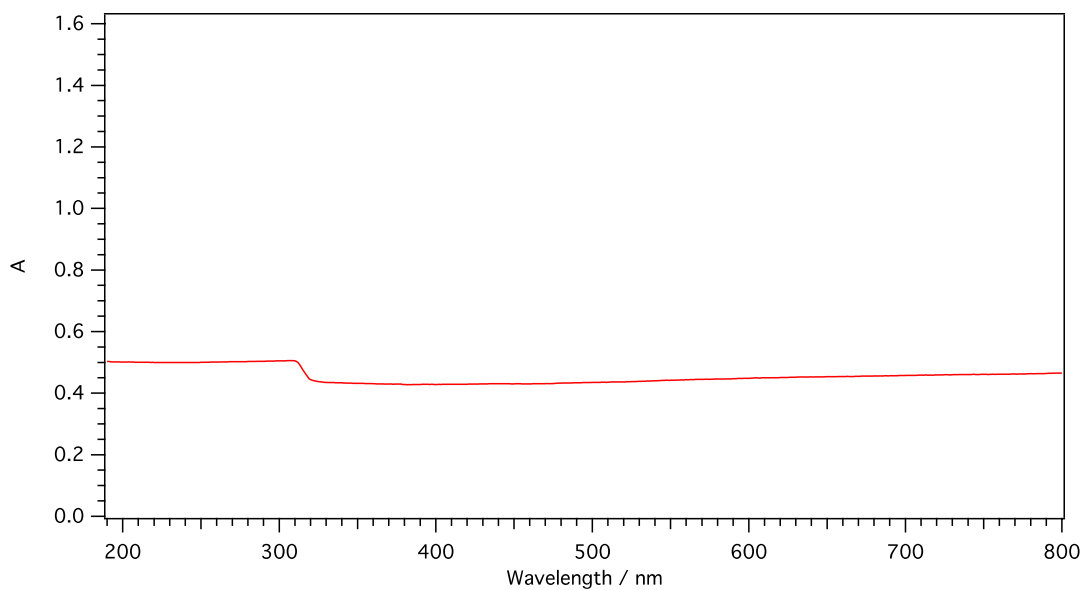


**Figure S41d.** Absorbance spectrum of gold micro-mesh electrode.

Compound	Colour (Wavelength / nm) <sup>a</sup>	Absorbance of Au micro-mesh <sup>b</sup>	Transmittance through Au micro-mesh ( $R_0$ ) <sup>c</sup>	Absorbance of compound + Au micro-mesh <sup>d</sup>	Transmission through compound + Au micro-mesh ( $R_x$ ) <sup>e</sup>	Chromatic contrast ratio: $R_0/R_x$ ( $c = 1$ mM)
<b>2</b>	Blue (612)	0.450	0.355	(0.777 + 0.450) = 1.227	0.059	6.0
<b>5</b>	Red (533)	0.439	0.364	(0.572 + 0.439) = 1.011	0.097	3.8
<b>9</b>	Green (732)	0.460	0.347	(0.541 + 0.460) = 1.001	0.100	3.5

**Table S1.** Table of chromatic contrast ratios measured at the gold micro-mesh electrode for 1 mM solutions of the analytes in CH<sub>3</sub>CN containing 0.2 M Bu<sub>4</sub>NPF<sub>6</sub>. <sup>a</sup>Wavelength used for measurement. <sup>b</sup>Absorbance of the gold micromesh electrode at specified wavelengths (from data in Figure S41d). <sup>c</sup>Equivalent transmission value from absorbance reading ( $T = 10^{-A}$ ). <sup>d</sup>Absorbance of compound plus absorbance of mesh (from data in Figures S41a-d) at specified wavelengths. <sup>e</sup>Equivalent transmission value from absorbance reading ( $T = 10^{-A}$ ).

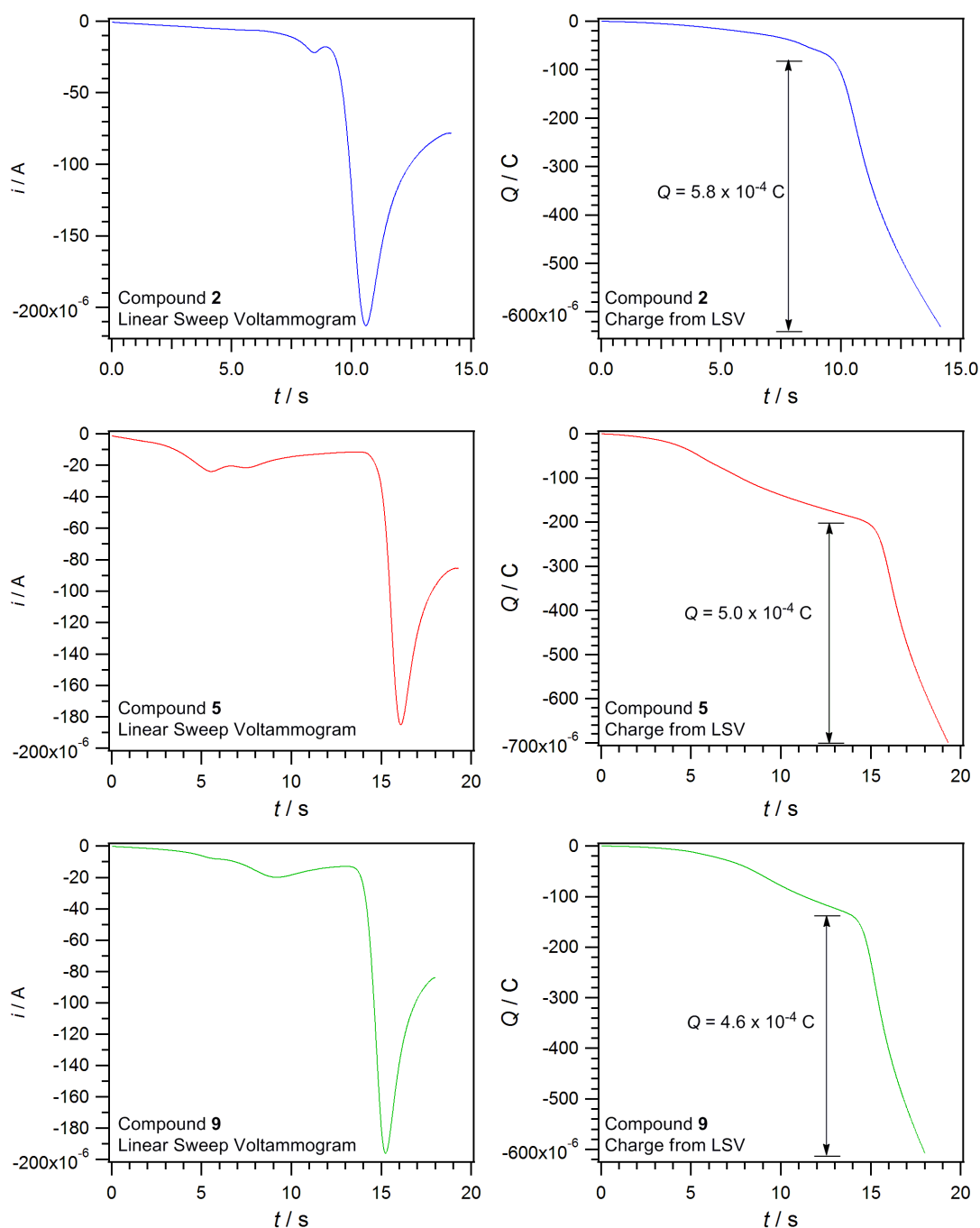


**Figure S42.** (Left hand side). Linear sweep voltammograms of compounds **2**, **5** and **9** in  $\text{CH}_3\text{CN}$  containing 0.2 M  $\text{Bu}_4\text{NPF}_6$  at the gold micro-mesh electrode. The  $x$ -axis has been converted from potential to time. (Right hand side) Integration of the current-time data in the left hand column to give the charge ( $Q$ ).

Compound	Colour (Wavelength / nm) <sup>a</sup>	Absorbance <sup>b</sup>	$Q / C^c$	Charge per unit area $Q_d / C \text{ cm}^{-2 d}$	Chromatic efficiencies: $\eta / \text{cm}^2 \text{ C}^{-1}$ ( $c = 1 \text{ mM}$ )
<b>2</b>	Blue (612)	0.777	$5.8 \times 10^{-4}$	$9.63 \times 10^{-4}$	800
<b>5</b>	Red (533)	0.572	$5.0 \times 10^{-4}$	$8.30 \times 10^{-4}$	690
<b>9</b>	Green (732)	0.541	$4.6 \times 10^{-4}$	$7.64 \times 10^{-4}$	430

**Table S2.** Table of chromatic efficiencies at the gold micro-mesh electrode for 1 mM solutions of the analytes in CH<sub>3</sub>CN containing 0.2 M Bu<sub>4</sub>NPF<sub>6</sub>. <sup>a</sup>Wavelength used for measurement. <sup>b</sup>Absorbance of the analyte at the specified wavelength (from data in Figures S41a-c). <sup>c</sup>Charge measured by integration of the current from linear sweep voltammetric measurements (from data in Figure S42). <sup>d</sup>Charge per unit area of electrode. The area of the electrode (0.6024 cm<sup>2</sup>) was estimated by the Randles-Sevcik equation ( $i_p = 2.686 \times 10^5 n^{3/2} A c D^{1/2} \nu^{1/2}$ ) using 1 mM ferrocene in acetonitrile solution as the standard and with a diffusion coefficient value of  $2.2 \times 10^{-5} \text{ cm}^2 \text{ s}^{-1}$ .

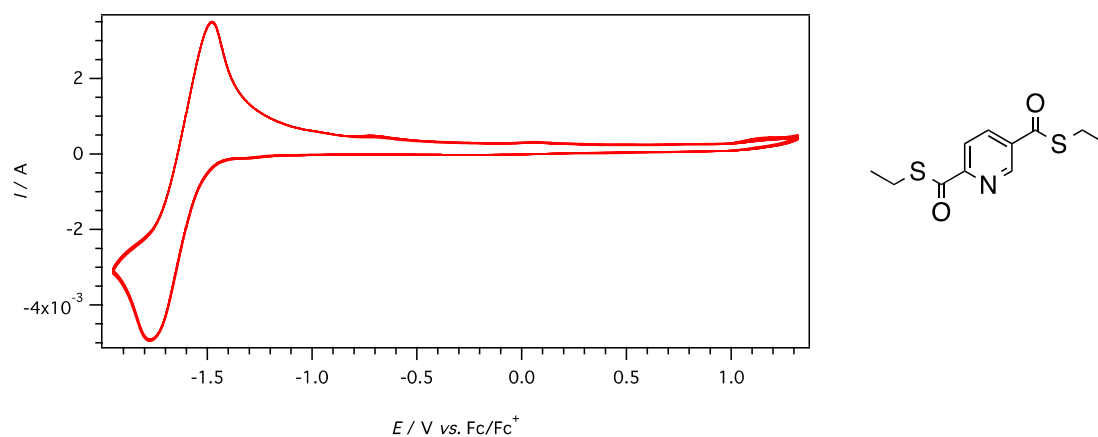


**Figure S43a:** Cyclic voltammograms (1<sup>st</sup>, 10<sup>th</sup>, 20<sup>th</sup>, 30<sup>th</sup>, 40<sup>th</sup>, 50<sup>th</sup>, 60<sup>th</sup>, 70<sup>th</sup>, 80<sup>th</sup>, 90<sup>th</sup>, 100<sup>th</sup>) of **2** at 20 °C. Scan rate ( $\nu$ ) at 0.9 V s<sup>-1</sup> obtained at a gold mesh electrode in CH<sub>3</sub>CN (0.2 M Bu<sub>4</sub>NPF<sub>6</sub>) for the 1-electron process over 100 cycles of *ca.* 10 mM analyte. Current data were scaled by multiplying by  $\nu^{0.5}$ .

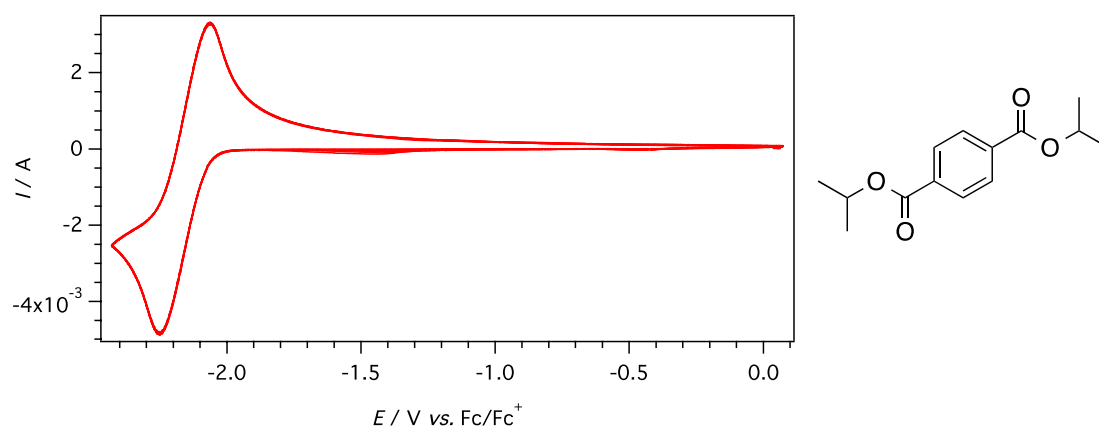


**Figure S43b:** Cyclic voltammograms (1<sup>st</sup>, 10<sup>th</sup>, 20<sup>th</sup>, 30<sup>th</sup>, 40<sup>th</sup>, 50<sup>th</sup>, 60<sup>th</sup>, 70<sup>th</sup>, 80<sup>th</sup>, 90<sup>th</sup>, 100<sup>th</sup>) of **5** at 20 °C. Scan rate ( $\nu$ ) at 0.5 V s<sup>-1</sup> obtained at a gold mesh electrode in CH<sub>3</sub>CN (0.2 M Bu<sub>4</sub>NPF<sub>6</sub>) for the 1-electron process over 100 cycles of *ca.* 10 mM analyte. Current data were scaled by multiplying by  $\nu^{-0.5}$ .

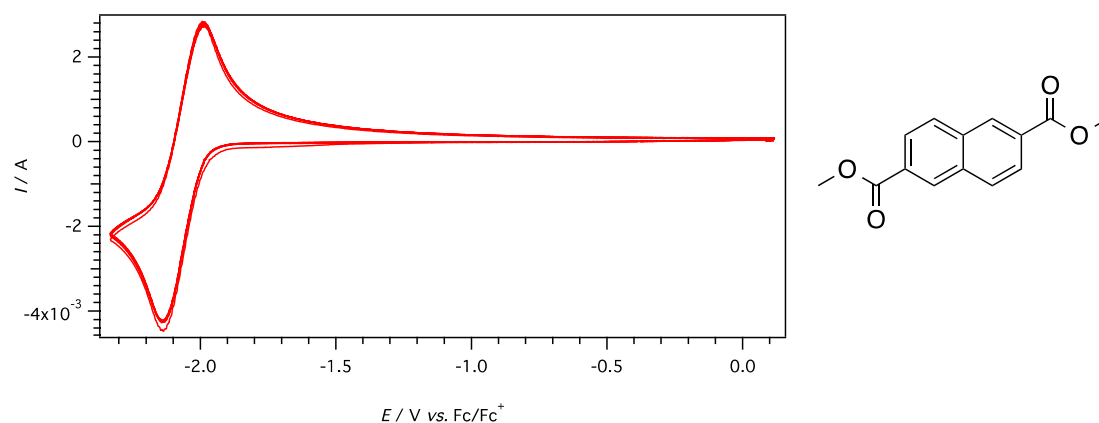


**Figure S43c:** Cyclic voltammograms (1<sup>st</sup>, 10<sup>th</sup>, 20<sup>th</sup>, 30<sup>th</sup>, 40<sup>th</sup>, 50<sup>th</sup>, 60<sup>th</sup>, 70<sup>th</sup>, 80<sup>th</sup>, 90<sup>th</sup>, 100<sup>th</sup>) of **9** at 20 °C. Scan rate ( $\nu$ ) at 0.5 V s<sup>-1</sup> obtained at a gold mesh electrode in CH<sub>3</sub>CN (0.2 M Bu<sub>4</sub>NPF<sub>6</sub>) for the 1-electron process over 100 cycles of *ca.* 10 mM analyte. Current data were scaled by multiplying by  $\nu^{-0.5}$ .